

### Roles of shati in METH-induced dopaminergic responses

The pharmacological effects of METH are linked to its capacity to elevate extracellular DA levels by releasing DA from presynaptic nerve terminals and inhibiting its reuptake (Heikkilä et al., 1975; Seiden et al., 1993). In addition, METH and the amphetamines redistribute DA from synaptic vesicles to the cytosol and promote reverse transport (Seiden et al., 1993). Therefore, we examined the effect of shati-AS on the METH-induced increase in overflow of DA in the NAc using an *in vivo* microdialysis technique. The experimental schedule is shown in Figure 6A. METH caused a marked increase in overflow of DA in the NAc of the CSF-treated mice on the day 3 (Fig. 6B). The peak of overflow of DA was increased by METH treatment to ~360% of the baseline level in the CSF-treated mice. In shati-AS-treated mice, the METH-induced increase in overflow of DA was significantly potentiated compared with that in the shati-SC- or CSF-treated mice (intracerebroventricular treatment,  $F_{(2,14)} = 5.662, p < 0.05$ ; time,  $F_{(10,140)} = 35.646, p < 0.01$ ; intracerebroventricular treatment  $\times$  time,  $F_{(20,140)} = 1.927, p < 0.05$ ; repeated ANOVA) (Fig. 6B). The levels of basal DA did not differ among the three groups.

Next, we examined the *in vivo* effect of shati-AS on [ $^3\text{H}$ ]DA uptake into synaptosomes in the midbrain. The experimental schedule is shown in Figure 6C. METH decreased [ $^3\text{H}$ ]DA uptake compared with the saline-treated mice. In shati-AS-treated mice, the METH-induced decrease in [ $^3\text{H}$ ]DA uptake was significantly potentiated compared with that in the shati-SC- or CSF-treated mice. Moreover, [ $^3\text{H}$ ]DA uptake in the saline-treated group was also decreased by shati-AS compared with that in the shati-SC- or CSF-treated mice, although shati-SC had no effect on [ $^3\text{H}$ ]DA uptake (drug,  $F_{(1,40)} = 30.447, p < 0.01$ ; intracerebroventricular treatment,  $F_{(2,40)} = 12.576, p < 0.01$ ; drug  $\times$  intracerebroventricular treatment,  $F_{(2,40)} = 0.392, p = 0.678$ ; two-way ANOVA) (Fig. 6D).

We also examined the *in vivo* effect of shati-AS on [ $^3\text{H}$ ]DA uptake into synaptic vesicle preparations in the midbrain, because the redistribution of DA from synaptic vesicles to cytoplasmic compartments through interaction with vesicular monoamine transporter-2 has been postulated to be primarily responsible for DA terminal injury by METH or amphetamines (Liu and Edwards, 1997; Uhl, 1998). METH decreased vesicular [ $^3\text{H}$ ]DA uptake compared with the saline-treated mice. In shati-AS-treated mice, the METH-induced decrease in vesicular [ $^3\text{H}$ ]DA uptake was significantly potentiated compared with that in the shati-SC- or CSF-treated mice. Moreover, [ $^3\text{H}$ ]DA uptake in the saline-treated group was also decreased by shati-AS compared with that in the shati-SC- or CSF-treated mice, although shati-SC had no effect on [ $^3\text{H}$ ]DA uptake (drug,  $F_{(1,42)} = 137.229, p < 0.01$ ; intracerebroventricular treatment,  $F_{(2,42)} = 15.087, p < 0.01$ ; drug  $\times$  intracerebroventricular treatment,  $F_{(2,42)} = 0.240, p = 0.788$ ; two-way ANOVA) (Fig. 6E).

Different results were obtained from *in vivo* microdialysis and DA uptake studies, only in the basal conditions. These studies were performed in quite different situations. Living mice were

used *in vivo* microdialysis study, and basal overflow of endogenous DA was measured 24 h after the last METH treatment in the NAc (Fig. 6B). Therefore, other factors (other neurotransmitters, neuroplasticity, and neuronal input from other brain regions) might affect basal DA overflow and compensate the dysfunction of DA uptake induced by repeated treatment of METH. Conversely, the experiment of [ $^3\text{H}$ ]DA uptake was *ex vivo* study by using the midbrain tissue (Fig. 6D,E). High-concentration and exogenous [ $^3\text{H}$ ]DA was used for the investigation of functional changes of DA uptake 1 h after the last METH treatment in the midbrain. The *ex vivo* method could more directly measure the changes of DA uptake in the midbrain, comparing *in vivo* microdialysis study.

### Roles of shati in METH-induced conditioned place preference

The effect of shati-AS on METH-induced CPP was examined in a place conditioning paradigm, in which animals learn the association of an environment paired with drug exposure. This paradigm involves sensory perception of external stimuli, association of stimuli, and the approach-inducing actions of a drug, as well as the rewarding effects of a drug. The experimental schedule is shown in Figure 7A. As shown in Figure 7B, METH (0.3 mg/kg, s.c.) produced place preference in mice. In shati-AS-treated mice, the development of METH-induced CPP was significantly potentiated compared with that in the shati-SC- or CSF-treated mice (drug,  $F_{(1,46)} = 78.202, p < 0.01$ ; intracerebroventricular treatment,  $F_{(2,46)} = 4.950, p = 0.011$ ; drug  $\times$  intracerebroventricular treatment,  $F_{(2,46)} = 5.046, p = 0.010$ ; two-way ANOVA) (Fig. 7B), indicating that downregulation of shati expression was sufficient to confer the enhanced METH-induced CPP. Shati-AS, shati-SC, or CSF treatment had no effect on CPP in saline-treated mice (Fig. 7B, left three columns), suggesting that the procedure in CPP might not reflect anxiolytic actions. These results suggest that shati participates in the repeated METH treatment-induced development of behavioral sensitization and CPP by regulating DA uptake.

### Discussion

In the present study, we identified a novel molecule shati from the NAc of mice treated with METH for the first time using the PCR-select cDNA subtraction method, which is a differential and epochal cloning technique.

From motif analysis of shati, shati contained the sequence of GCAT (Fig. 1C). Shati might have physiological action in producing acetylcholine or metabolic action of ATP, because the analysis showed the lowest interactive potential energy of shati with acetyl-CoA or ATP (supplemental Fig. 2, available at www.jneurosci.org as supplemental material). Accordingly, we have to investigate the mechanism by which shati regulates production of acetylcholine or metabolic roles of ATP in subsequent studies.

Because shati expression was detected at high levels in not only the brain regions related to drug dependence but also the liver, kidney, and spleen (Fig. 2A), it is plausible that shati is involved in the regulation of pathophysiological function. Single METH treatment induced the expression of shati mRNA in the NAc and Hip (Fig. 3C). Repeated METH treatment produces an enhancement of the locomotor-stimulating effects of METH (data not shown). Remarkable induction of shati mRNA expression was detected in the Fc, NAc, and CPU of the mice that

after METH treatment on the day 3. Values are means  $\pm$  SE ( $n = 8$ ). \* $p < 0.05$  versus saline-treated mice. <sup>a</sup> $p < 0.05$  versus shati-SC-treated mice. C, Experimental schedule for measurement of locomotor activity using shati-AS. D, Effect of shati-AS on repeated METH-induced behavioral sensitization. Mice were administered METH (1 or 2 mg/kg, s.c.) or saline for 5 d and challenged with METH (0.3 mg/kg, s.c.) on day 10. Locomotor activity was measured for 2 h on the days 1, 3, 5, and 10. Values are means  $\pm$  SE ( $n = 5-7$ ). ANOVA with repeated measures revealed significant differences in METH-induced sensitization (group,  $F_{(8,47)} = 51.238, p < 0.01$ ; day,  $F_{(2,94)} = 68.423, p < 0.01$ ; group  $\times$  day,  $F_{(16,94)} = 4.412, p < 0.01$ ). \* $p < 0.05$  versus METH plus CSF-treated mice. <sup>b</sup> $p < 0.05$  versus METH plus shati-SC-treated mice. <sup>c</sup> $p < 0.05$  versus the locomotor activity on day 1 in the same group.

showed behavioral sensitization to METH (Fig. 3A–C). There is strong evidence that the dopaminergic system, which projects from the VTA of the midbrain to the NAc and to other forebrain sites, including the Fc, dorsal striatum, and Hip, is a major substrate of reward and reinforcement for both natural rewards and addictive drugs (Di Chiara and Imperato, 1988; Robbins and Everitt, 1996; Wise, 1996a). Therefore, shati may be involved in the rewarding effects and reinforcement of addictive drugs. Because the dopaminergic neuronal system is involved primarily in the pharmacological effects of METH (Melega et al., 1995; Larsen et al., 2002; Sulzer et al., 2005), we examined whether the METH-induced increase in shati mRNA levels is mediated by the activation of dopaminergic neurotransmission. The METH-induced increase in the expression of shati mRNA in the NAc was completely inhibited by pretreatment with the DA D<sub>1</sub>-like receptor antagonist R(+)-SCH23390 and the DA D<sub>2</sub>-like receptor antagonist raclopride (Fig. 3D), suggesting that the activation of DA D<sub>1</sub> and D<sub>2</sub> receptors is attributable to METH-induced expression of shati. Behavioral studies have suggested that both DA D<sub>1</sub> and D<sub>2</sub> receptors mediate reinforcing signals for drug of abuse, because amphetamine-induced CPP and METH-induced sensitization are blocked by either DA D<sub>1</sub>-like or D<sub>2</sub>-like receptor antagonist (Ujike et al., 1989; Hiroi and White, 1991). Therefore, it likely that activation of DA transmission is necessary for METH-induced shati expression in neurons, in which shati specifically acts (Fig. 4A).

The contribution of dopaminergic transmission to behavioral sensitization and CPP has been well documented (Nakajima et al., 2004; Nagai et al., 2005a,b; Niwa et al., 2007a,b,d). Shati expression was upregulated by repeated administration of METH (Figs. 2B, 3, 4A), and downregulation of shati by AS (Figs. 4B, 5B) led to an elevated synaptic DA concentration in the NAc and major behavioral manifestations in mice: heightened locomotor activity (Fig. 5D), the rate of development of sensitization (Fig. 5D), and CPP (Fig. 7B) responding to METH. Furthermore, downregulation of shati expression by AS (Figs. 4B, 5B) potentiated the effects of METH on overflow of DA in the NAc (Fig. 6B) and DA uptake (Fig. 6D,E). These findings strongly suggest that the overexpression of shati elicited by METH may serve as a homeostatic mechanism that prevents hyperlocomotion

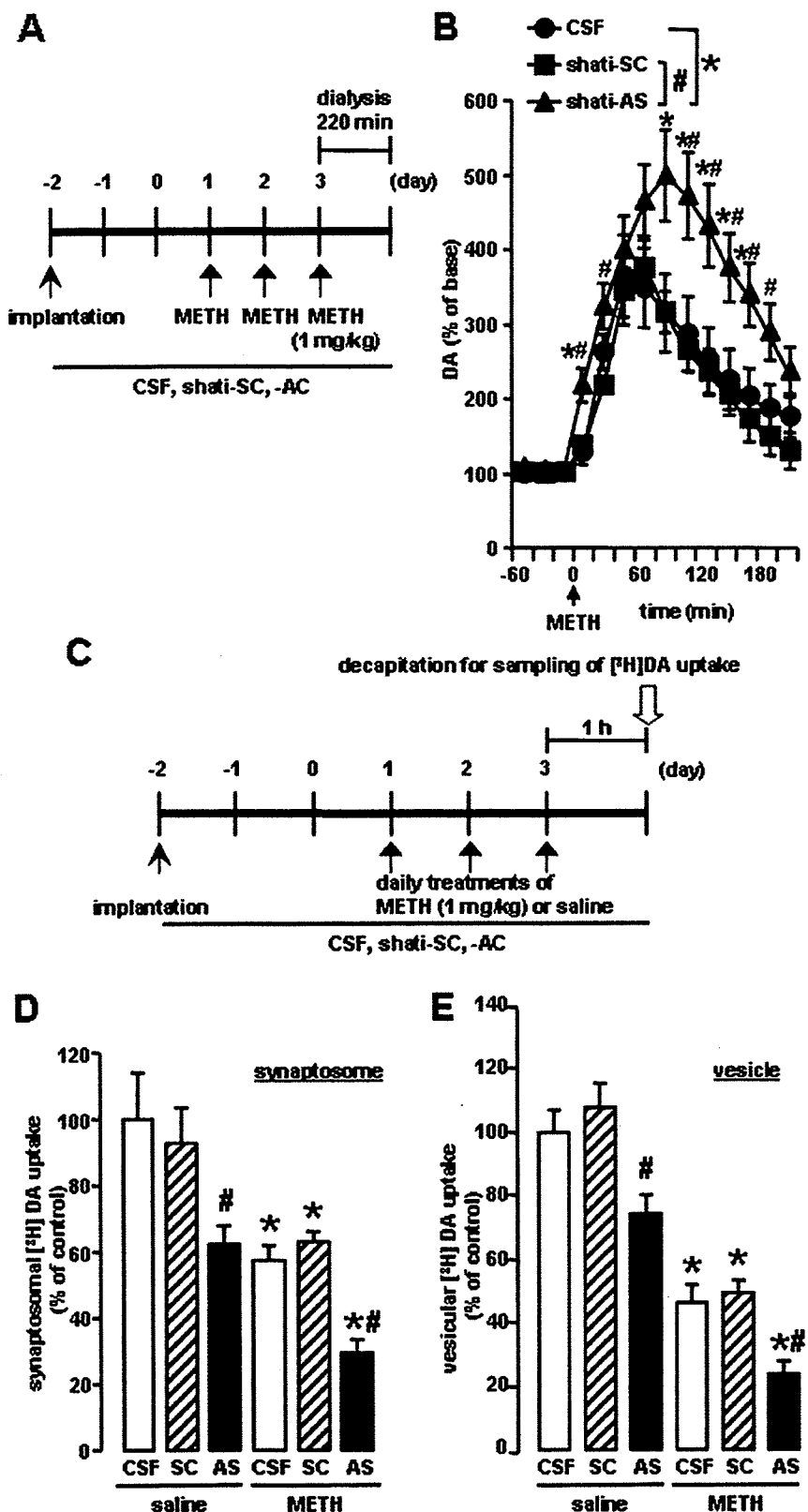


**Figure 6.** Effects of shati-AS on METH-induced dopaminergic responses. *A*, Experimental schedule for the measurement of overflow of DA using *in vivo* microdialysis using shati-AS. *B*, Effect of shati-AS on METH-induced increase in overflow of DA in the NAc. Mice were administered METH (1 mg/kg, s.c.) for 3 d. On day 3, levels of DA were measured in the NAc (AP +1.7 mm, ML –0.8 mm from bregma, and DV –4.0 mm from the skull) for 220 min after METH treatment by *in vivo* microdialysis. Basal levels of DA were  $0.30 \pm 0.08$ ,  $0.31 \pm 0.05$ , and  $0.30 \pm 0.04$  nM for the CSF-treated, shati-SC-treated, and shati-AS-treated mice, respectively. ANOVA with repeated measures revealed significant differences in METH-induced increase in overflow of DA (group,

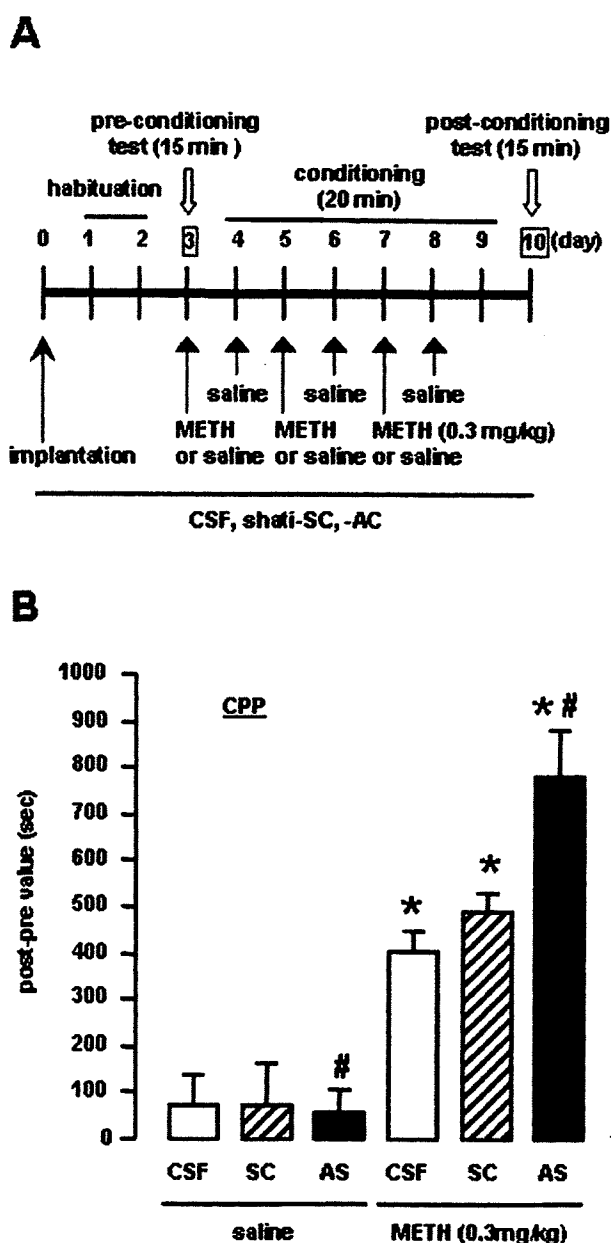


**Figure 7.** Effects of shati-AS on METH-induced conditioned place preference. **A**, Experimental schedule for the conditioned place preference task using shati-AS. **B**, Effect of shati-AS on METH-induced place preference. Mice were administered METH (0.3 mg/kg, s.c.) or saline during the conditioning for place preference. Values are means  $\pm$  SE ( $n = 5-12$ ). \* $p < 0.05$  versus saline-treated mice. # $p < 0.05$  versus shati-SC-treated mice.

$F_{(2,14)} = 5.662, p < 0.05$ ; time,  $F_{(10,140)} = 35.646, p < 0.01$ ; group  $\times$  time,  $F_{(20,140)} = 1.927, p < 0.05$ ). Values are means  $\pm$  SE ( $n = 5-6$ ). \* $p < 0.05$  versus CSF-treated mice. # $p < 0.05$  versus shati-SC-treated mice. **C**, Experimental schedule for the [ $^3$ H]DA uptake assay using shati-AS. **D**, Effect of shati-AS on METH-induced decrease of synaptosomal [ $^3$ H]DA uptake. Mice were administered METH (1 mg/kg, s.c.) for 3 d and decapitated 1 h after the last injection. The synaptosomal [ $^3$ H]DA uptake was  $0.32 \pm 0.04, 0.29 \pm 0.03, 0.20 \pm 0.02, 0.18 \pm 0.01, 0.20 \pm 0.01, 0.20 \pm 0.01$ , and  $0.09 \pm 0.01$  pmol/mg protein per 4 min for the saline plus CSF-treated, saline plus shati-SC-treated, saline plus shati-AS-treated, METH plus CSF-treated, METH plus shati-SC-treated, and METH plus shati-AS-treated mice, respectively. The final concentration of [ $^3$ H]DA was 5 nM. Values are means  $\pm$  SE ( $n = 7-8$ ). \* $p < 0.05$  versus saline-treated mice. # $p < 0.05$  versus shati-SC-treated mice. **E**, Effect of shati-AS on METH-induced decrease of vesicular [ $^3$ H]DA uptake. Mice were administered METH (1 mg/kg, s.c.) for 3 d and decapitated 1 h after the last injection. The vesicular [ $^3$ H]DA uptake was  $3.76 \pm 0.25, 4.05 \pm 0.29, 2.80 \pm 0.20, 1.74 \pm 0.21, 1.85 \pm 0.14$ , and  $0.90 \pm 0.14$  pmol/mg protein per 4 min for the saline plus CSF-treated, saline plus shati-SC-treated, saline plus shati-AS-treated, METH plus CSF-treated, METH plus shati-SC-treated, and METH plus shati-AS-treated mice, respectively. The final concentration of [ $^3$ H]DA was 30 nM. Values are means  $\pm$  SE ( $n = 8$ ). \* $p < 0.05$  versus saline-treated mice. # $p < 0.05$  versus shati-SC-treated mice.

tion, sensitization, and CPP, by promoting plasmalemmal and vesicular DA uptake as well as attenuating the METH-induced increase in overflow of DA in the NAc.

We used METH at the dose of 2 mg/kg for 6 d in the experiments of RT-PCR, real-time RT-PCR, and immunohistochemistry (Figs. 3, 4B–D, 5), because expression of shati was induced in the NAc of mice by METH (2 mg/kg for 6 d), which was detected by using a PCR-select cDNA subtraction method (supplemental Fig. 1, available at [www.jneurosci.org](http://www.jneurosci.org) as supplemental material). In AS experiments, shati-AS-treated mice tended to show a potentiation of METH (2 mg/kg)-induced hyperlocomotion and sensitization on days 1–5, but there were no statistically significant differences among the three groups (Fig. 5D). The dose-response effects of METH on the locomotor activity may reflect a shift to the left, but these effects were reached the plateau. Conversely, shati-AS-treated mice showed a marked potentiation of METH (1 mg/kg)-induced hyperlocomotion and sensitization on days 1–5 compared with shati-SC- or CSF-treated mice (Fig. 5D). On day 3, the potentiation of the METH-induced hyperlocomotion by shati-AS reached the maximum and plateau. Therefore, in the experiments of AS, we selected METH at the dose of 1 mg/kg for 3 d (Figs. 5B, 6B, D, E). We also confirmed that shati mRNA was increased by METH at the doses of 1 and 2 mg/kg for 3 d (Fig. 3A). Then, in the AS study, we selected METH at the dose of 1 mg/kg to investigate effects of AS.

We selected the time point of 2 h after the last METH treatment for the time when the animals were to be killed in the experiments of RT-PCR and real-time RT-PCR (Figs. 2, 3A, C, D), because expression of shati mRNA showed peak in the NAc of mice 2 h after the last METH treatment (Fig. 3B). We prepared the brain samples 24 h after the last METH treatment for immunohistochemical study (Fig. 4). The levels of shati mRNA in the NAc of mice treated with repeated METH were significantly increased 2, 6, and 24 h after the last METH treatment (Fig. 3B). At 24 h after the METH treatment, both transcription and translation of shati protein could be induced in the brain. Therefore, we considered that 24 h after the METH treatment is the best time point for investigation of shati protein expression.

Changes in mRNA and protein expression caused by drugs are of particular interest. The expression of certain mRNAs and proteins appears to be a compensatory adaptation to excessive DA signaling, which could be biologically significant adaptive mechanisms contributing to dependence. Nevertheless, some proteins play a reverse role. For example, we previously demonstrated that tPA potentiates METH- or MOR-induced rewarding and locomotor-stimulating effects (Nagai et al., 2004, 2005a, b), whereas TNF- $\alpha$  and its inducer inhibit them (Nakajima et al., 2004; Niwa et al., 2007a, b, d). The development of sensitization to amphetamine is prevented when an antibody that neutralized basic fibroblast growth factor (bFGF) is infused into the VTA before amphetamine treatment (Flores et al., 2000). Infusion of brain-derived neurotrophic factor (BDNF) into the NAc enhances the stimulation of locomotor activity by cocaine in rats, whereas the development of sensitization and CPP is delayed in heterozygous BDNF knock-out mice compared with wild-type littermates (Horger et al., 1999; Hall et al., 2003). Infusion of GDNF into the VTA blocks certain biochemical adap-

tations to chronic cocaine treatment (induction of tyrosine hydroxylase, NR1 subunit of NMDA receptors,  $\Delta$ FosB, and protein kinase A catalytic subunit) as well as cocaine-induced rewarding effects (Messer et al., 2000). Conversely, responses to cocaine are enhanced in rats by intra-VTA infusion of anti-GDNF antibody and in GDNF heterozygous knock-out mice (Messer et al., 2000). A partial reduction in the expression of GDNF potentiates METH self-administration, enhances motivation to take METH, increases vulnerability to drug-primed reinforcement, and prolongs cue-induced reinforcement of extinguished METH-seeking behavior (Yan et al., 2007). cAMP response element-binding protein (CREB) overexpression in the NAc reduces the rewarding properties of cocaine, whereas expression of a dominant-negative form of CREB in this region has the opposite effect (Carlezon et al., 1998; Walters and Blendy, 2001; McClung and Nestler, 2003). Furthermore, *FosB* mutant mice shows exaggerated locomotor activation in response to initial cocaine exposures as well as robust CPP to a lower dose of cocaine compared with wild-type littermates (Hiroi et al., 1997). Changes in the balance of levels between proaddictive factors, such as bFGF, tPA, and BDNF, and anti-addictive factors, such as TNF- $\alpha$ , GDNF, CREB, and *FosB*, induced by drugs of abuse seems to be important to the development of drug dependence. In the present study, the facilitation of METH-induced behavioral sensitization in mice with a targeted downregulation of shati highlights the opposing role of shati in drug-dependent behavioral plasticity. Therefore, upregulation of shati expression may represent a homeostatic response of dopaminergic neurons in the NAc to excessive dopaminergic transmission, resulting in attenuation of hypersensitivity and CPP induced by METH-like drugs. Our findings, together with others, suggest that there are molecules in the brain that normally inhibit the behavioral actions of addictive substances. The mechanism underlying the upregulation of shati caused by METH remains to be elucidated; nevertheless, inhibitory feedback of the excessive DA signaling is likely to be a plausible candidate.

In conclusion, the present study established a functional interaction between shati and METH. Our findings suggest that shati is involved in the development of METH-induced hyperlocomotion, sensitization, and CPP, by promoting plasmalemmal and vesicular DA uptake as well as attenuating the METH-induced increase in overflow of DA in the NAc.

## References

- Ang E, Chen J, Zagouras P, Magna H, Holland J, Schaeffer E, Nestler EJ (2001) Induction of nuclear factor- $\kappa$ B in nucleus accumbens by chronic cocaine administration. *J Neurochem* 79:221–224.
- Blackshaw S, Harpavat S, Trimarchi J, Cai L, Huang H, Kuo WP, Weber G, Lee K, Fraioli RE, Cho SH, Yung R, Asch E, Ohno-Machado L, Wong WH, Cepko CL (2004) Genomic analysis of mouse retinal development. *PLoS Biol* 2:E247.
- Bowers MS, McFarland K, Lake RW, Peterson YK, Lapish CC, Gregory ML, Lanier SM, Kalivas PW (2004) Activator of G protein signaling 3: a gatekeeper of cocaine sensitization and drug seeking. *Neuron* 42:269–281.
- Carlezon Jr WA, Thome J, Olson VG, Lane-Ladd SB, Brodtkin ES, Hiroi N, Duman RS, Neve RL, Nestler EJ (1998) Regulation of cocaine reward by CREB. *Science* 282:2272–2275.
- Cha XY, Pierce RC, Kalivas PW, Mackler SA (1997) NAC-1, a rat brain mRNA, is increased in the nucleus accumbens three weeks after chronic cocaine self-administration. *J Neurosci* 17:6864–6871.
- Christensen AV, Arnt J, Hyytel J, Larsen JJ, Svendsen O (1984) Pharmacological effects of a specific dopamine D-1 antagonist SCH 23390 in comparison with neuroleptics. *Life Sci* 34:1529–1540.
- Diatchenko L, Lau YF, Campbell AP, Chenchik A, Moqadam F, Huang B, Lukyanov S, Lukyanov K, Gurskaya N, Sverdlov ED, Siebert PD (1996) Suppression subtractive hybridization: a method for generating differentially regulated or tissue-specific cDNA probes and libraries. *Proc Natl Acad Sci USA* 93:6025–6030.
- Di Chiara G, Imperato A (1988) Drugs abused by humans preferentially increase synaptic dopamine concentrations in the mesolimbic system of freely moving rats. *Proc Natl Acad Sci USA* 85:5274–5278.
- Douglass J, Daoud S (1996) Characterization of the human cDNA and genomic DNA encoding CART: a cocaine- and amphetamine-regulated transcript. *Gene* 169:241–245.
- Erickson JD, Masserano JM, Barnes EM, Ruth JA, Weiner N (1990) Chloride ion increases [ $^3$ H]dopamine accumulation by synaptic vesicles purified from rat striatum: inhibition by thiocyanate ion. *Brain Res* 516:155–160.
- Fleckenstein AE, Metzger RR, Wilkins DG, Gibb JW, Hanson GR (1997) Rapid and reversible effects of methamphetamine on dopamine transporters. *J Pharmacol Exp Ther* 282:834–838.
- Flores C, Samaha AN, Stewart J (2000) Requirement of endogenous basic fibroblast growth factor for sensitization to amphetamine. *J Neurosci* 20:RC55(1–5).
- Franklin KBJ, Paxinos G (1997) The mouse brain: in stereotaxic coordinates. San Diego: Academic.
- Giros B, Jaber M, Jones SR, Wightman PM, Caron MG (1996) Hyperlocomotion and indifference to cocaine and amphetamine in mice lacking the dopamine transporter. *Nature* 379:606–612.
- Gurskaya NG, Diatchenko L, Chenchik A, Siebert PD, Khaspekov GL, Lukyanov KA, Vagner LL, Ermolaeva OD, Lukyanov SA, Sverdlov ED (1996) Equalizing cDNA subtraction based on selective suppression of polymerase chain reaction: cloning of Jurkat cell transcripts induced by phytohemagglutinin and phorbol 12-myristate 13-acetate. *Anal Biochem* 240:90–97.
- Hall FS, Drgonova J, Goeb M, Uhl GR (2003) Reduced behavioral effects of cocaine in heterozygous brain-derived neurotrophic factor (BDNF) knockout mice. *Neuropsychopharmacology* 28:1485–1490.
- Heikkilä RE, Orlansky H, Cohen G (1975) Studies on the distinction between uptake inhibition and release of  $^3$ H-dopamine in rat brain tissue slices. *Biochem Pharmacol* 24:847–852.
- Hiroi N, White NM (1991) The amphetamine conditioned place preference: differential involvement of dopamine receptor subtypes and two dopaminergic terminal areas. *Brain Res* 552:141–152.
- Hiroi N, Brown JR, Haile CN, Ye H, Greenberg ME, Nestler EJ (1997) FosB mutant mice: loss of chronic cocaine induction of Fos-related proteins and heightened sensitivity to cocaine's psychomotor and rewarding effects. *Proc Natl Acad Sci USA* 94:10397–10402.
- Horger BA, Iyasere CA, Berhow MT, Messer CJ, Nestler EJ, Taylor JR (1999) Enhancement of locomotor activity and conditioned reward to cocaine by brain-derived neurotrophic factor. *J Neurosci* 19:4110–4122.
- Koob GF (1992) Drugs of abuse: anatomy, pharmacology and function of reward pathways. *Trends Pharmacol Sci* 13:177–184.
- Koob GF, Sanna PP, Bloom FE (1998) Neuroscience of addiction. *Neuron* 21:467–476.
- Laakso A, Mohn AR, Gainetdinov RR, Caron MG (2002) Experimental genetic approaches to addiction. *Neuron* 36:213–228.
- Larsen KE, Fon EA, Hastings TG, Edwards RH, Sulzer D (2002) Methamphetamine-induced degeneration of dopaminergic neurons involves autophagy and upregulation of dopamine synthesis. *J Neurosci* 22:8951–8960.
- Liu Y, Edwards RH (1997) The role of vesicular transporter proteins in synaptic transmission and neural degeneration. *Annu Rev Neurosci* 20:125–156.
- Lorrain DS, Arnold GM, Vezina P (2000) Previous exposure to amphetamine increases incentive to obtain the drug: long-lasting effects revealed by the progressive ratio schedule. *Behav Brain Res* 107:9–19.
- McClung CA, Nestler EJ (2003) Regulation of gene expression and cocaine reward by CREB and  $\Delta$ FosB. *Nat Neurosci* 6:1208–1215.
- Melega WP, Williams AE, Schmitz DA, DiStefano EW, Cho AK (1995) Pharmacokinetic and pharmacodynamic analysis of the actions of D-amphetamine and D-methamphetamine on the dopamine terminal. *J Pharmacol Exp Ther* 274:90–96.
- Messer CJ, Eisch AJ, Carlezon Jr WA, Whisler K, Shen L, Wolf DH, Westphal H, Collins F, Russell DS, Nestler EJ (2000) Role for GDNF in biochemical and behavioral adaptations to drugs of abuse. *Neuron* 26:247–257.
- Mizoguchi H, Yamada K, Mizuno M, Mizuno T, Nitta A, Noda Y, Nabeshima T (2004) Regulations of methamphetamine reward by extracellular

- signal-regulated kinase 1/2/ets-like gene-1 signaling pathway via the activation of dopamine receptors. *Mol Pharmacol* 65:1293–1301.
- Mizoguchi H, Yamada K, Niwa M, Mouri A, Mizuno T, Noda Y, Nitta A, Itoharu S, Banno Y, Nabeshima T (2007) Reduction of methamphetamine-induced sensitization and reward in matrix metalloproteinase-2 and -9-deficient mice. *J Neurochem* 100:1579–1588.
- Nagai T, Yamada K, Yoshimura M, Ishikawa K, Miyamoto Y, Hashimoto K, Noda Y, Nitta A, Nabeshima T (2004) The tissue plasminogen activator-plasmin system participates in the rewarding effect of morphine by regulating dopamine release. *Proc Natl Acad Sci USA* 101:3650–3655.
- Nagai T, Noda Y, Ishikawa K, Miyamoto Y, Yoshimura M, Ito M, Takayanagi M, Takuma K, Yamada K, Nabeshima T (2005a) The role of tissue plasminogen activator in methamphetamine-related reward and sensitization. *J Neurochem* 92:660–667.
- Nagai T, Kamei H, Ito M, Hashimoto K, Takuma K, Nabeshima T, Yamada K (2005b) Modification by the tissue plasminogen activator-plasmin system of morphine-induced dopamine release and hyperlocomotion, but not anti-nociceptive effect in mice. *J Neurochem* 93:1272–1279.
- Nagai T, Ito M, Nakamichi N, Mizoguchi H, Kamei H, Fukakusa A, Nabeshima T, Takuma K, Yamada K (2006) The rewards of nicotine: regulation by tissue plasminogen activator-plasmin system through protease activated receptor-1. *J Neurosci* 26:12374–12383.
- Nakajima A, Yamada K, Nagai T, Uchiyama T, Miyamoto Y, Mamiya T, He J, Nitta A, Mizuno M, Tran MH, Seto A, Yoshimura M, Kitaichi K, Hasegawa T, Saito K, Yamada Y, Seishima M, Sekikawa K, Kim HC, Nabeshima T (2004) Role of tumor necrosis factor- $\alpha$  in methamphetamine-induced drug dependence and neurotoxicity. *J Neurosci* 24:2212–2225.
- Napier TC, Givens BS, Schulz DW, Bunney BS, Breese GR, Mailman RB (1986) SCH23390 effects on apomorphine-induced responses of nigral dopaminergic neurons. *J Pharmacol Exp Ther* 236:838–845.
- Nestler EJ (2001) Molecular basis of long-term plasticity underlying addiction. *Nat Rev Neurosci* 2:119–128.
- Nestler EJ (2002) From neurobiology to treatment: progress against addiction. *Nat Neurosci* 5:1076–1079.
- Niwa M, Nitta A, Shen L, Noda Y, Nabeshima T (2007a) Involvement of glial cell line-derived neurotrophic factor in inhibitory effects of a hydrophobic dipeptide Leu-Ile on morphine-induced sensitization and rewarding effects. *Behav Brain Res* 179:167–171.
- Niwa M, Yamada K, Yamada Y, Nakajima A, Saito K, Seishima M, Shen L, Noda Y, Furukawa S, Nabeshima T (2007b) An inducer for glial cell line-derived neurotrophic factor and tumor necrosis factor- $\alpha$  protects against methamphetamine-induced rewarding effects and sensitization. *Biol Psychiatry* 61:890–901.
- Niwa M, Nitta A, Yamada K, Nabeshima T (2007c) The roles of glial cell line-derived neurotrophic factor, tumor necrosis factor- $\alpha$ , and an inducer of these factors in drug dependence. *J Pharmacol Sci*, in press.
- Niwa M, Nitta A, Yamada Y, Nakajima A, Saito K, Seishima M, Noda Y, Nabeshima T (2007d) Tumor necrosis factor- $\alpha$  and its inducer inhibit morphine-induced rewarding effects and sensitization. *Biol Psychiatry*, in press.
- Noda Y, Miyamoto Y, Mamiya T, Kamei H, Furukawa H, Nabeshima T (1998) Involvement of dopaminergic system in phencyclidine-induced place preference in mice pretreated with phencyclidine repeatedly. *J Pharmacol Exp Ther* 286:44–51.
- Robbins TW, Everitt BJ (1996) Neurobehavioural mechanisms of reward and motivation. *Curr Opin Neurobiol* 6:228–236.
- Robinson TE, Berridge KC (1993) The neural basis of drug craving: an incentive-sensitization theory of addiction. *Brain Res Brain Res Rev* 18:247–291.
- Satel SL, Southwick SM, Gawin FH (1991) Clinical features of cocaine-induced paranoia. *Am J Psychiatry* 148:495–498.
- Schechter MD, Calcagnetti DJ (1998) Continued trends in the conditioned place preference literature from 1992 to 1996, inclusive, with a cross-indexed bibliography. *Neurosci Biobehav Rev* 22:827–846.
- Seiden LS, Sabol KE, Ricaurte GA (1993) Amphetamine: effects on catecholamine systems and behavior. *Annu Rev Pharmacol Toxicol* 33:639–677.
- Strakowski SM, Sax KW (1998) Progressive behavioral response to repeated d-amphetamine challenge: further evidence for sensitization in humans. *Biol Psychiatry* 44:1171–1177.
- Strausberg RL, Feingold EA, Grouse LH, Derge JG, Klausner RD, Collins FS, Wagner L, Shenmen CM, Schuler GD, Altschul SF, Zeeberg B, Buetow KH, Schaefer CF, Bhat NK, Hopkins RF, Jordan H, Moore T, Max SI, Wang J, Hsieh F et al. (2002) Generation and initial analysis of more than 15,000 full-length human and mouse cDNA sequences. *Proc Natl Acad Sci USA* 99:16899–16903.
- Sulzer D, Sonders MS, Poulsen NW, Galli A (2005) Mechanisms of neurotransmitter release by amphetamines: a review. *Prog Neurobiol* 75:406–433.
- Taubenfeld SM, Milekic MH, Monti B, Alberini CM (2001) The consolidation of new but not reactivated memory requires hippocampal C/EBP $\beta$ . *Nat Neurosci* 4:813–818.
- Uhl GR (1998) Hypothesis: the role of dopaminergic transporters in selective vulnerability of cells in Parkinson's disease. *Ann Neurol* 43:555–560.
- Ujike H, Onoue T, Akiyama K, Hamamura T, Otsuki S (1989) Effects of selective D-1 and D-2 dopamine antagonists on development of methamphetamine-induced behavioral sensitization. *Psychopharmacology* 98:89–92.
- Wada R, Tiff CJ, Proia RL (2000) Microglial activation precedes acute neurodegeneration in Sandhoff disease and is suppressed by bone marrow transplantation. *Proc Natl Acad Sci USA* 97:10954–10959.
- Walters CL, Blendy JA (2001) Different requirements for cAMP response element binding protein in positive and negative reinforcing properties of drugs of abuse. *J Neurosci* 21:9438–9444.
- Wang XB, Funada M, Imai Y, Revay RS, Ujike H, Vandenberg DJ, Uhl GR (1997) rG $\beta$ 1: a psychostimulant-regulated gene essential for establishing cocaine sensitization. *J Neurosci* 17:5993–6000.
- Wise RA (1996a) Addictive drugs and brain stimulation reward. *Annu Rev Neurosci* 19:319–340.
- Wise RA (1996b) Neurobiology of addiction. *Curr Opin Neurobiol* 6:243–251.
- Wolf ME (1998) The role of excitatory amino acids in behavioral sensitization to psychomotor stimulants. *Prog Neurobiol* 54:679–720.
- Yamada K, Nabeshima T (2004) Pro- and anti-addictive neurotrophic factors and cytokines in psychostimulant addiction: mini review. *Ann NY Acad Sci* 1025:198–204.
- Yan Y, Yamada K, Niwa M, Nagai T, Nitta A, Nabeshima T (2007) Enduring vulnerability to reinstatement of methamphetamine-seeking behavior in glial cell line-derived neurotrophic factor mutant mice. *FASEB J*, in press.
- Zachariou V, Bolanos CA, Selley DE, Theobald D, Cassidy MP, Kelz MB, Shaw-Lutchman T, Berton O, Sim-Selley LJ, Dileone RJ, Kumar A, Nestler EJ (2006) An essential role for  $\Delta$ FosB in the nucleus accumbens in morphine action. *Nat Neurosci* 9:205–211.

## ORIGINAL ARTICLE

# Identification of Piccolo as a regulator of behavioral plasticity and dopamine transporter internalization

X Cen<sup>1,2</sup>, A Nitta<sup>1</sup>, D Ibi<sup>1,3</sup>, Y Zhao<sup>1</sup>, M Niwa<sup>1</sup>, K Taguchi<sup>1</sup>, M Hamada<sup>1</sup>, Y Ito<sup>3</sup>, Y Ito<sup>4</sup>, L Wang<sup>2</sup> and T Nabeshima<sup>1,5</sup>

<sup>1</sup>Department of Neuropsychopharmacology and Hospital Pharmacy, Nagoya University Graduate School of Medicine, Nagoya, Japan; <sup>2</sup>National Chengdu Center for Safety Evaluation of Drugs, West China Hospital, Sichuan University, Chengdu, China; <sup>3</sup>Department of Pharmacology, College of Pharmacy, Nihon University, Chiba, Japan; <sup>4</sup>Equipment Center for Research and Education, Nagoya University Graduate School of Medicine, Nagoya, Japan and <sup>5</sup>Department of Chemical Pharmacology, Meijo University Graduate School of Pharmaceutical Sciences, Nagoya, Japan

Dopamine transporter (DAT) internalization is a mechanism underlying the decreased dopamine reuptake caused by addictive drugs like methamphetamine (METH). We found that Piccolo, a presynaptic scaffolding protein, was overexpressed in the nucleus accumbens (NAc) of the mice repeatedly administrated with METH. Piccolo downexpression by antisense technique augmented METH-induced behavioral sensitization, conditioned reward and synaptic dopamine accumulation in NAc. Expression of Piccolo C<sub>2</sub>A domain attenuated METH-induced inhibition of dopamine uptake in PC12 cells expressing human DAT. Consistent with this, it slowed down the accelerated DAT internalization induced by METH, thus maintaining the presentation of plasmalemmal DAT. In immunostaining and structural modeling Piccolo C<sub>2</sub>A domain displays an unusual feature of sequestering membrane phosphatidylinositol 4,5-bisphosphate, which may underlie its role in modulating DAT internalization. Together, our results indicate that Piccolo upregulation induced by METH represents a homeostatic response in the NAc to excessive dopaminergic transmission. Piccolo C<sub>2</sub>A domain may act as a cytoskeletal regulator for plasmalemmal DAT internalization, which may underlie its contributions in behavioral plasticity.

*Molecular Psychiatry* (2008) 13, 451–463; doi:10.1038/sj.mp.4002132; published online 15 January 2008

**Keywords:** Piccolo; dopamine transporter; methamphetamine; behavioral plasticity; C<sub>2</sub>A domain

## Introduction

Dopamine transporter (DAT), a member of the Na<sup>+</sup>/Cl<sup>-</sup>-dependent transporters in the dopaminergic neurons, is critical for terminating dopamine (DA) neurotransmission and contributes to the abuse potential of psychostimulants. The stimulating and reinforcing effects of drugs result from enhanced synaptic DA accumulation in specific brain areas like nucleus accumbens (NAc). Cocaine and methamphetamine (METH; or its analogue amphetamine) elevate extracellular DA by inhibiting DA reuptake through DAT and, in the case of METH, also by promoting reverse transport of nonvesicular DA, reducing plasma membrane DAT through internalization, and displacing DA from synaptic vesicle (SV) to the cytoplasm.<sup>1,2</sup>

Membrane trafficking of DAT is closely associated with DA homeostasis and synaptic plasticity, and increasing evidences have showed that METH-like drugs are able to modulate this dynamic process.<sup>3</sup> The internalization of plasmalemmal DAT is a clathrin-mediated process,<sup>4,5</sup> and internalized DAT can be sorted to endosomal compartments where they may be recycled to cell surface and/or lysosome for degradation.<sup>6</sup> Inhibition of endocytic machinery assembly can attenuate amphetamine- or phorbol ester-mediated DAT internalization,<sup>7</sup> whereas expression of endosomal proteins like Rab5 in endosomal vesicles promotes amphetamine-induced intracellular DAT accumulation.<sup>8</sup> These findings strongly suggest that manipulation of endocytic components could be an important manner for regulating DAT internalization.

Piccolo, a component of the presynaptic cytoskeletal matrix, is assembled ultrastructurally as an electron-dense region of filaments at the active zone (AZ). It is proposed to play a scaffolding role in regulating AZ assembly,<sup>9</sup> actin cytoskeleton and SV trafficking.<sup>10,11</sup> Piccolo contains multiple subdomains including PDZ domain and Ca<sup>2+</sup>/phospholipid binding (C<sub>2</sub>A and C<sub>2</sub>B) domains, each of which exhibits

Correspondence: Professor T Nabeshima, Department of Chemical Pharmacology, Meijo University Graduate School of Pharmaceutical Sciences, 150 Yagotoyama, Tenpaku, Nagoya 468-8503, Japan.

E-mail: tnabeshi@ccmfs.meijo-u.ac.jp

Received 17 June 2007; revised 14 September 2007; accepted 21 September 2007; published online 15 January 2008

distinctive features.<sup>10,12</sup> PDZ domain may interact with other presynaptic molecules involving molecule anchoring and assembly at AZ.<sup>13</sup> C<sub>2</sub>A domain shows an unusual ability to sense intracellular changes of Ca<sup>2+</sup> levels and then trigger the association with membrane phospholipids (PIs) via electrostatic interaction.<sup>14</sup> Notably, it interacts with phosphatidylinositol 4,5-bisphosphate (PIP<sub>2</sub>),<sup>15</sup> a critical molecule for actin dynamics and endocytosis. It is well established that PIP<sub>2</sub> coordinates membrane fusion with actin filament to promote membrane movement, and recruits accessory adaptors for clathrin-coated pits.<sup>16</sup> Therefore, modulation of plasmalemmal PIP<sub>2</sub> may affect PIP<sub>2</sub>-dependent biological processes like membrane trafficking and endocytosis.

In this study we find that Piccolo serves as a negative presynaptic modulator for behavioral hypersensitivity and blunts excessive dopaminergic synaptic plasticity by regulating plasmalemmal DAT internalization. Moreover, Piccolo C<sub>2</sub>A domain may contribute to such distinct effects by targeting membrane PIP<sub>2</sub>.

## Materials and methods

### Material

A pCMV-hDAT expression plasmid was kindly provided by Dr Marc Caron (Duke University Medical Center). The expression plasmids of pCMV-HA-Piccolo-PDZ (amino acid 3900–4244), pCMV-Myc-Piccolo-C<sub>2</sub>A (amino acid 4704–5610) and pGEX4T-GST-p13192 (amino acid 4364–4755; named p13192) were constructed as previously described.<sup>17</sup> The following antibodies were used: hDAT and tyrosine hydroxylase (TH; Chemicon International Inc., Billerica, MA); hemagglutinin epitope (HA) and c-Myc (Cell Signaling, Billerica, MA); GST (Amersham Biosciences, Uppsala, Sweden); Piccolo and Rim 2 (Synaptic Systems, Albany, OR); PIP<sub>2</sub> (Assay Designs, Ann Arbor, MI, USA); syntaxin 1A (Santa Cruz Biotechnology, Santa Cruz, CA); synaptophysin (Sigma-Aldrich, St Louis, MO). The following reagents were used: botulinum neurotoxin (Bont)/C1 and Bont/B (Wako Pure Chemical Industries Ltd, Osaka, Japan); sulfo-NHS-biotin and immobilized streptavidin (Pierce, Rockford, IL).

### RT-PCR and real-time RT-PCR

Isolation of total RNA from the NAc of mice was performed using RNeasy Mini Kit (QIAGEN, Hilden, Germany). The mRNA productions from nine target cDNA sequences of Piccolo were assayed by reverse transcription (RT)-PCR, followed by electrophoresis. The forward and reverse primers for the nine sequences were shown in Supplementary Table 1. Piccolo mRNA levels in brain NAc were validated by quantitative real-time RT-PCR using an iCycler System (Bio-Rad, Hercules, CA). Briefly, isolation of total RNA was performed using RNeasy Mini Kit (QIAGEN). For reverse transcription, 1 µg RNA was converted into a cDNA by a standard 20 µl reverse

transcriptase reaction using oligo (dT) primers (Invitrogen, Hercules, CA) and Superscript II RT (Bio-Rad Laboratories, Hercules, CA, USA). Total cDNA (1 µl) was amplified in a 25 µl reaction mixture using 0.1 µM each of forward and reverse primers and Platinum Quantitative PCR SuperMix-UDG (Invitrogen). The primer and dye probes were designed by Nippon Gene Co. Ltd (Tokyo, Japan) using Primer Express software. The forward primer was 5'-GGATAGCGCACAAAGGTTTTCC-3' (base pair 4180–4200) with reverse being 5'-TTCAACCGAATCATAGGATGCTC-3' (base pair 4257–4279), and the dye probe was 5'-CACAAAGAGAATCCTGAGCTGGTCGATGA-3' (base pair 4192–4220). Ribosomal mRNA was used and determined as control for RNA integrity with TaqMan ribosomal RNA control reagents.

### Antisense

An antisense oligodeoxynucleotide (AS; 5'-CTCTGCCAAAACCTTC-3') and a scramble oligodeoxynucleotide (SC; 5'-AACGTAGTCACGTAG-3') were synthesized by Nippon Gene Co. Ltd. C57BL/6 mice were infused intracerebroventricularly with AS or SC (1 µl h<sup>-1</sup>, 10 nmol ml<sup>-1</sup>), made in regular artificial cerebrospinal fluid (CSF) or CSF alone, using an implanted Alzet minipump (AP -0.5 mm, ML +1.0 mm from bregma, DV -2.0 mm from the skull).

### Locomotor activity and CPP Test

Locomotor activity was measured using an infrared detector (Neuroscience, Tokyo, Japan) as our previous report.<sup>18</sup> The mice were injected with METH (1 mg kg<sup>-1</sup>, s.c.) daily for 5 days (day 1–5), followed by locomotor activity measurement at days 1, 3 and 5. Conditioned place-preference (CPP) test was carried out according to the methods as described before but with modification in conditioning.<sup>19</sup> Briefly, a mouse was allowed to move freely between transparent and black boxes for 20 min once per day for 3 days (from day 2 to day 0) in the preconditioning. In the mornings from days 1 to 3, the mouse was treated with METH (1 mg kg<sup>-1</sup>, s.c.) and put in nonpreferred box for 20 min. After an interval of 12 h the mouse was treated with saline and put in the side opposite to the METH-conditioning box for 20 min. On day 4, the post-conditioning test was performed without drug treatment, and place-conditioning behavior was expressed as post-value minus pre-value.

### Microdialysis

C57BL/6 mice were anesthetized before a guide cannula was implanted in the NAc (AP +1.7 mm, ML -0.8 mm from bregma, DV -4.0 mm from the skull).<sup>19</sup> Meanwhile, a mini osmotic pump filled with AS, SC (10 nmol ml<sup>-1</sup>) or CSF was implanted intracerebroventricularly as described above. Equal numbers of animals were assigned to METH and saline pretreatment groups. Dialysis probes were inserted to the guide cannula the night prior to the experiment. Microdialysis samples were collected every 10 min (2.0 µl min<sup>-1</sup>). The DA output was presented as



relative to the baseline (the average concentration of four consecutive stable samples defined as 100%).

#### Western blotting and immunostaining

To determine expression of Piccolo, brain tissue or cell lysate was solubilized in homogenization buffer (150 mM NaCl, 1 mM EDTA, 10 mM Tris, 100 mM Na<sub>2</sub>CO<sub>3</sub>, pH 11.5) with a mixture of protease inhibitor. After shaking for 30 min and centrifugation at 4 °C, supernatants were subjected to SDS-PAGE (4% polyacrylamide) and transferred to polyvinylidene difluoride membranes. Mouse brains or cultured cells were fixed in 4% paraformaldehyde in PBS and permeabilized with 0.4% Triton X-100.

#### Cell culture, transfection and [<sup>3</sup>H]DA uptake

PC12 cells (Riken Bioresource Center Cell Bank, Tsukuba, Japan) were cultured on polyornithine-coated culture coverslips in Dulbecco's modified Eagle's medium (DMEM) supplemented with 10% heat-inactivated horse serum and 5% fetal bovine serum (FBS).<sup>6</sup> For stable expression of hDAT, PC12 cells were transfected with pCMV-hDAT using Lipofectamine 2000 (Invitrogen). A stably transfected pool was selected with 800 µg ml<sup>-1</sup> geneticin (Invitrogen). For transient expression, the cells were transfected with the plasmids expressing different domain of Piccolo. The primary cultured dopaminergic neurons were separated from ventral midbrains of rat embryos (day 14). [<sup>3</sup>H]DA uptake in hDAT-PC12 cells was performed as described before.<sup>20</sup> Briefly, cells were washed in Krebs-Ringers-HEPES (KRH) buffer twice before assay. Uptake was initiated by adding 1 µM 3, 4-(ring-2,5,6-<sup>3</sup>H)-DA (Perkin Elmer, Waltham, MA) containing 10<sup>-5</sup> M pargyline and 10<sup>-5</sup> M ascorbic acid. Uptake proceeded for 10 min at 23 °C and was terminated by three rapid washes in ice-cold KRH buffer. Accumulated [<sup>3</sup>H]DA was determined by liquid scintillation counting (Beckman LS6500). Nonspecific uptake was defined in the presence of 10 µM GBR12909 (Sigma).

#### Cell-surface biotinylation and internalization assays

Biotinylation internalization assays were performed as described previously.<sup>6</sup>

#### Structural models

Molecule models of Piccolo C<sub>2</sub>A domain were generated using the amino-acid sequence data from Protein Data Bank (Gi:42543545). The C<sub>2</sub>A domain models were energy minimized using Molecular Operating Environment (MOE) software (Chemical Computing Group, Montreal, Canada) to fix any mismatches between the various structural segments. All calculations used an MMFF94x force field and a cutoff distance of 9.5 Å for nonbinding interactions. ASEDock of the MOE program was used for phospholipids and/or Ca<sup>2+</sup> ions docking stimulation. DSviewer Lite software (Accelry Inc., San Diego, USA) was used for modeling of the electrostatic surface.

#### Statistics

All data were expressed as means ± s.e.m. Statistical significance was determined by a one-way ANOVA, followed by the Bonferroni-Dunn test for multigroup comparisons. Differences were considered significant when *P* < 0.05.

#### Results

##### Overexpression of Piccolo in the NAc of METH-treated mice

The reasons for pursuing Piccolo for intensive investigation arose from our preliminary findings in PCR-select cDNA subtraction strategy (Clontech Laboratories, Palo Alto, CA, USA) for detecting the

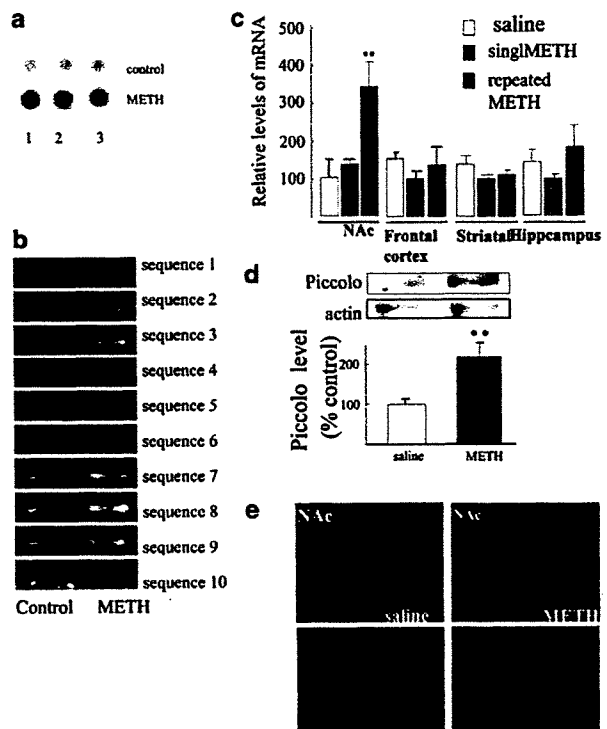


**Figure 1** Piccolo expression in nucleus accumbens (NAc) was upregulated by repeated methamphetamine (METH) administration. (a) Piccolo overexpression in the NAc of a representative mouse after daily METH administration for 5 days was shown. (b) RT-PCR analysis revealed a significant increase in the productions of the target sequences of Piccolo induced by METH. (c) Piccolo mRNA production was elevated significantly in NAc, rather than in the frontal cortex, striatal and hippocampus, of the mice treated with repeated METH. Data are expressed as percent of mRNA level of NAc in saline-treated mice (*n* = 6). \*\**P* < 0.01, compared with saline or single dosing of METH (in NAc). (d) Western blotting analysis showed the elevation of Piccolo level in NAc responding to repeated METH. \*\**P* < 0.01, compared with saline. (e) Immunostaining showed the elevation of Piccolo immunoreactivity in the NAc of the mice administrated with repeated METH. Saline-treated mice (left column) and METH-treated mice (right column).



affected genes in the NAc by METH. The C57BL/6J mice were daily administrated with METH ( $2 \text{ mg kg}^{-1}$ , s.c.) for 5 days, and Piccolo mRNA production in the NAc was found to increase by 240% in comparison to that of saline-treated mice (Figure 1a). Although little is known about the function of Piccolo in drug-induced behavioral sensitization, its subcellular localization, molecular functions and interacting partners led us to presume that Piccolo overexpression elicited by METH could be involved in DA signaling strength and presynaptic plasticity.

We performed a series of experiments to validate the results from PCR-select cDNA subtraction. After the mice were daily administrated with METH ( $1 \text{ mg kg}^{-1}$ , s.c.) for 5 days, Piccolo mRNA levels in the NAc were measured semiquantitatively by RT-PCR. As Piccolo possesses several splicing domain structures, we amplified and analyzed 10 different target sequences. As shown in Figure 1b, repeated METH administration significantly elevated the mRNA productions of the target sequences of Piccolo in NAc. To confirm such alterations, the mRNA productions of Piccolo in different brain regions were measured quantitatively by real-time RT-PCR 2 h after single METH dosing ( $1 \text{ mg kg}^{-1}$ , s.c.) or the final injection of daily METH administration ( $1 \text{ mg kg}^{-1}$ , s.c.) for 5 days. As shown in Figure 1c, the levels of Piccolo mRNA in the frontal cortex, striatal or hippocampus were not affected by either single or repeated METH administration. Remarkably, Piccolo mRNA level in the NAc was increased following repeated METH administration ( $F_{(2,15)} = 5.58$ ;  $P < 0.05$ ), whereas it was not altered by single METH injection. We then examined Piccolo expression in the NAc using western blotting. Consistently, Piccolo protein level in NAc was elevated apparently after repeated METH administration ( $t_{(1,8)} = 7.35$ ;  $P < 0.01$ ; Figure 1d). Immunostaining also revealed a strengthened Piccolo immunoreactivity in NAc of the mice treated with repeated METH (Figure 1e). Taken together, our data suggest a selective increase of Piccolo expression in NAc of behaviorally sensitized mice induced by repeated METH dosing, rather than a global increase of the brain. Because NAc is a brain area closely associated with drug dependence, we presumed that Piccolo overexpression may be involved in dopaminergic plasticity in neural circuits, which is critical for reward.

#### *Piccolo modulates behavioral plasticity and synaptic DA concentration in NAc*

To correlate Piccolo expression with the behavioral and neurochemical phenotype to METH, we utilized an AS strategy, which has been widely used to manipulate gene expressions in the brain via intracerebroventricular infusion.<sup>21</sup> The designed AS, which directs against nucleotides 2452–2466, has been demonstrated to downregulate successfully the expression of Piccolo in previous studies.<sup>17</sup> Additionally, a SC was used as a control.

The mice were infused continuously with AS, SC or CSF using implanted osmotic minipumps for 3 days before daily saline or METH administration ( $1 \text{ mg kg}^{-1}$ , s.c.) for 5 days. Such infusion was sustained till the end of each behavioral test. Locomotor activities of mice were measured at days 1, 3 and 5 immediately after drug injection (Figure 2a). There was no difference among Piccolo AS-, SC- or CSF-treated mice in baseline locomotor activity throughout a 30 min habituation period (data not shown) or in response to saline (Figure 2b). Repeated METH administration caused a progressive hyperlocomotion in mice, and interestingly, AS-pretreated mice developed a greater hyperlocomotor activity than those treated with SC or CSF after METH administration for 3 days ( $F_{(2,15)} = 5.47$ ;  $P < 0.05$ ; Figure 2c). Furthermore, such enhanced hyperlocomotor activity was sustained till day 5 despite that the difference was not significant compared with that of SC- or CSF-pretreated mice.

We then investigated the potential role of Piccolo in the rewarding effects by the CPP, a classical conditioning paradigm in which animals learn to prefer an environment associated with drug exposure. The mice were infused with AS, SC or CSF for 3 days before the training of CPP (Figure 2d). As shown in Figure 2e, the CSF-treated mice showed baseline preference for either side of the test chambers prior to METH administration, and developed the significant place conditioning after training with METH ( $F_{(5,42)} = 9.12$ ;  $P < 0.05$ ). Notably, the Piccolo AS-pretreated mice showed approximately a double degree of place conditioning compared to those treated with SC or CSF, indicating that the AS-treated mice developed an enhancement of rewarding effect to METH. The mice were killed immediately after the behavioral test to measure Piccolo protein levels in NAc. Piccolo expression in NAc responding to METH was dramatically increased, whereas AS effectively decreased its expression (Figure 2f). These results indicate that Piccolo downregulation was sufficient to confer METH-enhanced sensitization and rewarding effect, which is mediated predominantly by the dopaminergic system. No evidence of neurotoxicity in pathological histology was found outside of the mechanical disruption produced by implantation of the infusion cannula in our experimental conditions (data not shown).

We finally measured DA release in the NAc by a microdialysis technique. The mice were infused with Piccolo AS, SC or CSF for 3 days before daily METH administration ( $1 \text{ mg kg}^{-1}$ , s.c.) for 3 days (Figure 2g). The basal levels of DA in NAc did not differ among CSF-, AS- or SC-treated mice (CSF,  $0.58 \pm 0.21 \text{ nM}$ ; AS,  $0.49 \pm 0.17 \text{ nM}$ ; SC,  $0.60 \pm 0.18 \text{ nM}$ ) before the final challenge of METH. As expected, DA levels in the NAc were markedly increased immediately after the final challenge of METH. Obviously, AS pretreatment promoted METH-induced DA release in the NAc compared with SC or CSF ( $F_{(2,9)} = 5.874$ ;  $P < 0.05$ ; Figure 2h). These data strongly supported

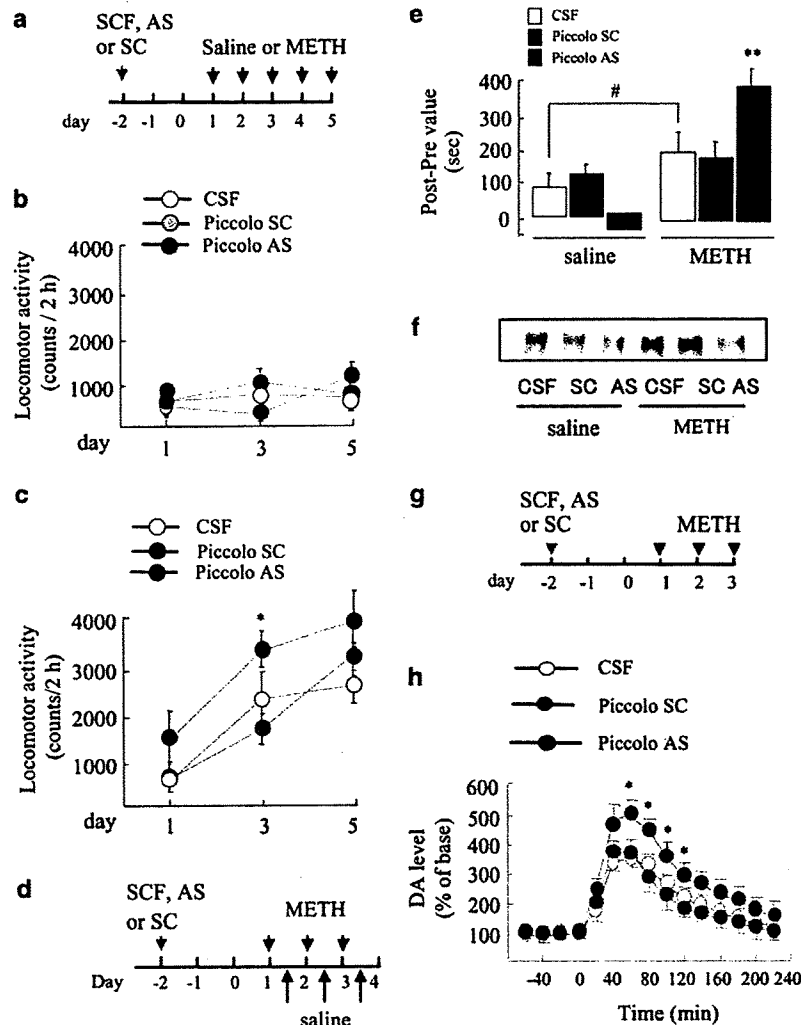


**Figure 2** Downregulation of Piccolo expression with antisense oligodeoxynucleotide (AS) promoted methamphetamine (METH)-induced behavioral and synaptic plasticity. (a–c) Mice were infused intracerebroventricularly with Piccolo AS, scramble oligodeoxynucleotide (SC) or cerebrospinal fluid (CSF) for 3 days before daily saline (b) or METH (c) administration for 5 days. Locomotor activities were measured at days 1, 3 and 5 ( $n=6$ ).  $*P<0.05$ , compared with SC or CSF. (d, e) Mice were infused with Piccolo AS, SC or CSF for 3 days before conditioned place-preference (CPP) training. On day 4, the post-conditioning test was performed ( $n=8$ ).  $**P<0.01$ , compared with SC or CSF in METH-treated groups,  $*P<0.05$ , compared with CSF in saline-treated group. (f) The representative immunoblots from western blotting indicated that Piccolo expression in the nucleus accumbens (NAc) was inhibited by AS in the mice treated by repeated METH. (g, h) Mice were infused with AS, SC or CSF for 3 days, followed by daily METH administration for 3 days. Microdialysis was conducted after the final METH injection ( $n=4$ ).  $*P<0.05$ , compared with SC or CSF at the same time point.

the findings in behavioral tests, suggesting that the enhanced accumulation of DA in NAc resulted from AS may contribute to the amplified responsiveness to METH; moreover, Piccolo may play a role in modulating synaptic DA concentration. Taken these results together, Piccolo overexpression in NAc may present a mechanism of opposing the behavioral responsiveness to METH.

*Piccolo is colocalized in dopaminergic neurons*

To study whether Piccolo is expressed in dopaminergic neurons, double immunostaining was performed in primary cultured dopaminergic neurons. The

immunoreactivities of Piccolo and TH revealed an extensive overlap along neuronal projections, indicating that Piccolo is present at dopaminergic synapse (Figure 3a). Notably, abundant Piccolo immunoreactivity was observed as clusters and puncta at the dopaminergic terminals (Figure 3b). Moreover, we also found that almost all of the DAT-immunopositive clusters were present at Piccolo-containing clusters situated along dendritic profiles (Figure 3c), implying the potential interplay of these two molecules. These results strongly support the conclusion that Piccolo is a shared component of the dopaminergic synapses.

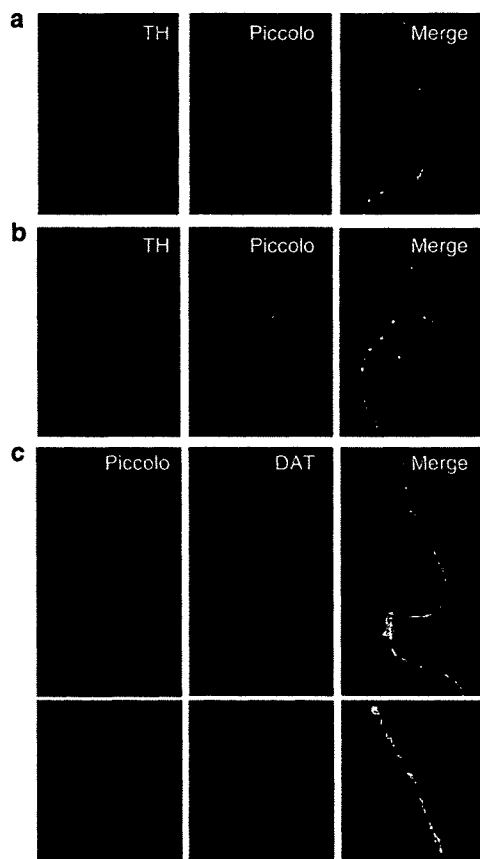


**Figure 3** Expression of Piccolo in dopaminergic neurons. (a) Double immunostaining showed that Piccolo is expressed in tyrosine hydroxylase (TH)-positive neurons. (b) Abundant expression of Piccolo is present at the presynaptic component of cultured dopaminergic neurons. (c) Dopamine transporter (DAT) immunoreactivity along the dendritic profiles is paralleled with that of Piccolo.

*Piccolo C<sub>2</sub>A domain attenuates the inhibition of DA uptake induced by METH through modulating plasmalemmal DAT expression*

Total DAT expression levels showed no changes when hDAT-PC12 cells were exposed to either METH (1  $\mu$ M) for various time periods or concentrations for 30 min (Figures 4a and b). However, the level of cell surface hDAT was reduced in time-dependent manner, and importantly, such reduction was paralleled with the extent of the inhibition of [<sup>3</sup>H]DA uptake ( $F_{(4,15)} = 25.6$ ,  $P < 0.001$ ; Figure 4c). Similar results were also obtained in dose-dependent studies, which showed a good correlation of the level of surface hDAT and [<sup>3</sup>H]DA uptake responding to various concentrations of METH ( $F_{(4,15)} = 73.0$ ,  $P < 0.001$ ; Figure 4d).

The schematic representations of C<sub>2</sub>A domain, PDZ domain and a fragment between C<sub>2</sub>A domain and PDZ domain are shown in Figure 4e. The C<sub>2</sub>A domain, PDZ domain or the fragment were expressed in hDAT-PC12 cells to investigate the changes in [<sup>3</sup>H]DA uptake. We found that the cells transfected

with C<sub>2</sub>A domain showed a slight, but not significant, increase in [<sup>3</sup>H]DA uptake in response to saline; moreover, transfection of PDZ domain or p13192 did not alter [<sup>3</sup>H]DA uptake, either (Figure 4f, left panel). We then pretreated the cells with 1  $\mu$ M METH for 30 min, followed by [<sup>3</sup>H]DA uptake assay. METH obviously inhibited [<sup>3</sup>H]DA uptake, and importantly, C<sub>2</sub>A domain-transfected cells showed a higher level of [<sup>3</sup>H]DA uptake compared with empty pCMV (Stratagene, La Jolla, CA;  $F_{(3,20)} = 18.68$ ,  $P < 0.01$ ), indicating that the C<sub>2</sub>A domain expression could attenuate METH-induced inhibition of DA uptake (Figure 4f, right panel).

Because an increase in DA uptake could be resulted from more DAT molecules expressed at the cell surface, we introduced these vectors into hDAT-PC12 cells, and analyzed plasmalemmal hDAT expression by cell-surface biotinylation. The expression levels of cell-surface hDAT did not increase significantly after transfection of C<sub>2</sub>A domain, PDZ domain or p13192 in basal conditions (Figure 4g). When the cells were pretreated with 1  $\mu$ M METH for 30 min, C<sub>2</sub>A domain transfection significantly attenuated the decrease in cell surface hDAT level compared to pCMV ( $F_{(3,8)} = 14.61$ ,  $P < 0.01$ ), whereas PDZ domain and p13192 showed no effects (Figure 4h). Such change was consistent with that of [<sup>3</sup>H]DA uptake shown in Figure 4f, indicating that Piccolo C<sub>2</sub>A domain may attenuate the METH-induced inhibition of DA uptake and maintain DAT expression at cell surface.

*Piccolo C<sub>2</sub>A domain modulates DAT internalization by a mechanism of membrane association*

Given that DAT can be internalized and/or recycled, we speculated that the decreased loss of membrane DAT induced by METH in C<sub>2</sub>A domain-transfected cells could be resulted from attenuated DAT internalization. To test this hypothesis, DAT internalization was measured by reversible biotinylation in hDAT-PC12 cells. We found that C<sub>2</sub>A domain expression could not affect the basal DAT internalization, as revealed by the similar amount of internalized DAT among all groups (Figure 5a). However, DAT internalization was significantly attenuated by C<sub>2</sub>A domain expression when the cells were exposed to 1  $\mu$ M METH for 30 min ( $F_{(3,8)} = 8.55$ ,  $P < 0.01$ ; Figure 5b). Expression of both PDZ domain and p13192 failed to affect the basal or METH-induced DAT internalization. Double immunostaining for hDAT and c-Myc-tagged C<sub>2</sub>A domain showed the similar findings that the cells transfected with C<sub>2</sub>A domain still maintained a strong plasmalemmal hDAT immunoreactivity responding to METH, whereas a relatively large amount of internalized hDAT was observed in cytosolic compartments of the cells transfected with empty pCMV (Figure 5c). These results indicated that Piccolo C<sub>2</sub>A domain attenuates METH-induced DAT internalization, which accounts for the decrease in the loss of DAT at cell surface.

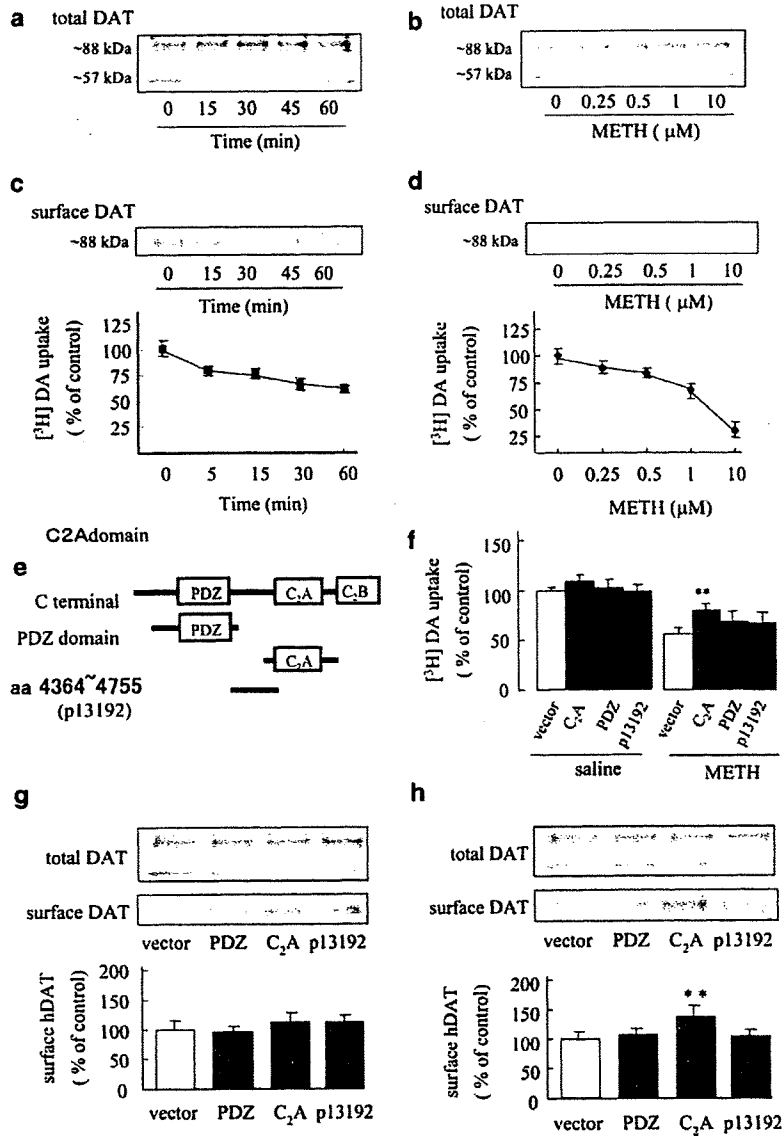


**Figure 4** Piccolo C<sub>2</sub>A domain increased dopamine (DA) uptake and dopamine transporter (DAT) surface expression. (a, b) Methamphetamine (METH) could not alter the total DAT expression levels in hDAT-PC12 cells in both time- (a) and dose-dependent studies (b). (c) METH (1 μM) decreased plasmalemmal DAT expression (top) in time-dependent manner, which was paralleled with the decrease in [<sup>3</sup>H]DA uptake (bottom). \*\**P* < 0.01, compared with the basal level. (d) METH decreased DAT expression at the cell surface dose-dependently (top), which was consistent with the decrease in [<sup>3</sup>H]DA uptake (bottom). \*\**P* < 0.01 and \**P* < 0.05, compared with the basal level. (e) Schematic representations of C<sub>2</sub>A domain, PDZ domain and a fragment (amino acid 4364–4755). (f) Piccolo C<sub>2</sub>A domain attenuated the METH-induced inhibition of [<sup>3</sup>H]DA uptake (right panel), but failed to change the basal DA uptake (left panel) (*n* = 6). \*\**P* < 0.01, compared with pCMV. (g, h) Piccolo C<sub>2</sub>A domain could not influence DAT surface expression in hDAT-PC12 cells responding to saline (g). However, it attenuated METH-induced loss of surface DAT (h). \*\**P* < 0.01, compared with pCMV in METH-treated group.

To study the potential mechanism underlying the action of Piccolo C<sub>2</sub>A domain on DAT internalization, we introduced C<sub>2</sub>A domain into hDAT-PC12 cells and then analyzed membrane subcellular distributions of Piccolo, C<sub>2</sub>A domain, hDAT as well as PIP<sub>2</sub>. The cells were homogenized in regular RIPA buffer containing 1% Triton-X 100, and separated into a soluble supernatant and a particulate membrane fraction (120 000 g,

60-min pellet). The latter was solubilized again in RIPA buffer or RIPA buffer containing 0.1 M Na<sub>2</sub>CO<sub>3</sub> (pH 11.5), which can extract a major part of detergent-resistant Piccolo protein from brain tissues.<sup>12</sup> As shown in Figure 5d, Piccolo, Piccolo C<sub>2</sub>A domain and PIP<sub>2</sub> did not fractionate like a soluble cytosolic protein but was mainly found in membrane sediment extracted by Na<sub>2</sub>CO<sub>3</sub>, indicating that a substantial

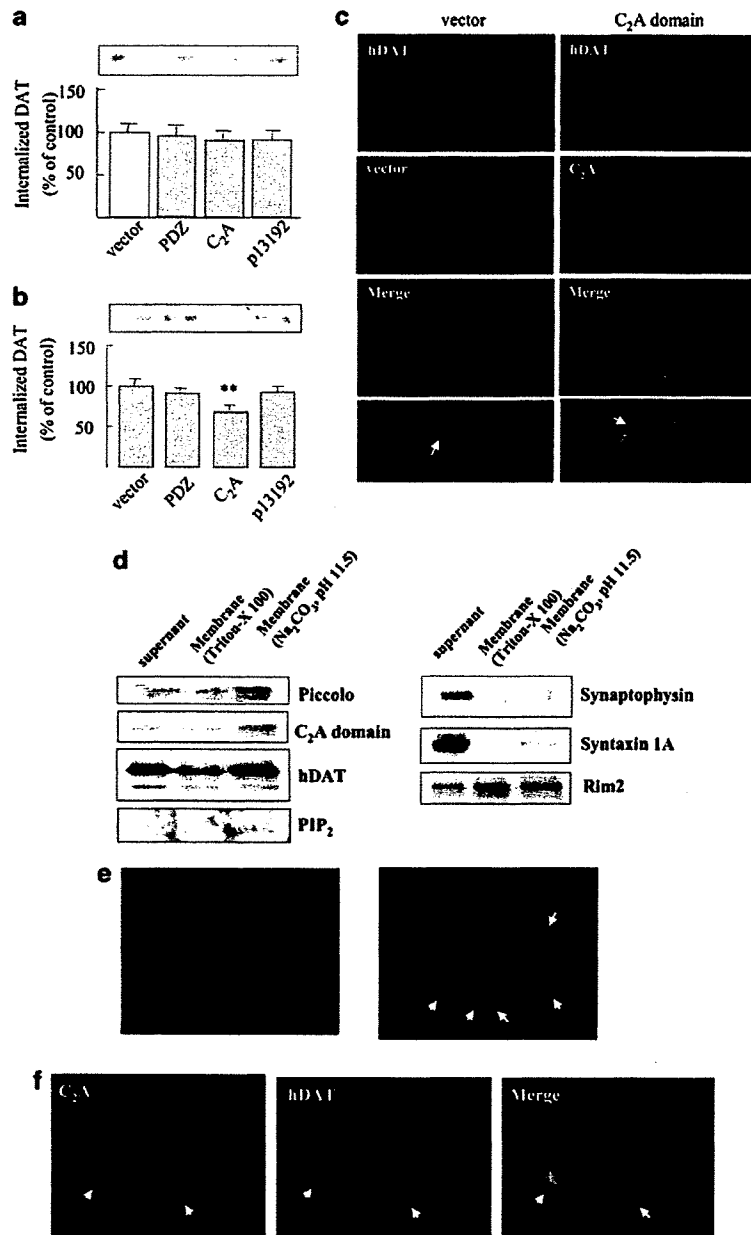


**Figure 5** Piccolo modulates dopamine transporter (DAT) internalization by a mechanism of membrane association. (a, b) After transfection with various vectors the hDAT-PC12 cells were biotinylated and treated with either saline (a) or 1 μM methamphetamine (METH) (b) for 30 min to initiate endocytosis. Top, representative blots of internalized hDAT. Bottom, quantitation of hDAT immunoreactivity.  $P < 0.01$ , compared with empty vector (pCMV) in METH-treated group. (c) The internalization of hDAT (red) was triggered by exposure of 1 μM METH for 30 min. The cells transfected with empty vector (pCMV) show enriched internalized hDAT (left panel), whereas the cells transfected with c-Myc-tagged-C<sub>2</sub>A domain (green) reveal the strong plasmalemmal hDAT immunoreactivity (right panel). Internalized hDAT is depicted. (d) Distributions of Piccolo, c-Myc-tagged C<sub>2</sub>A domain, hDAT, PIP<sub>2</sub> and other presynaptic proteins in hDAT-PC12 cells. The cells and membrane fractions were extracted with RIPA buffer containing 0.1 M Na<sub>2</sub>CO<sub>3</sub> (pH 11.5) or not. (e) The transfected Piccolo C<sub>2</sub>A domain specially targets plasma membrane in hDAT-PC12 cells. (f) Piccolo C<sub>2</sub>A domain shows a paralleled immunoreactivity pattern at plasmalemmal rafts with hDAT (arrowhead).

fraction of membrane-bound Piccolo, C<sub>2</sub>A domain and PIP<sub>2</sub> are associated with the same plasmalemmal rafts. Interestingly, a significant amount of hDAT was also recovered in both soluble fraction and membrane

sediment extracted by Na<sub>2</sub>CO<sub>3</sub>, indicating that a relatively major part of membrane DAT is localized at the same subcellular fraction with Piccolo C<sub>2</sub>A domain and PIP<sub>2</sub>. The similar distributions of these

components in lipid raft fractions hint that C<sub>2</sub>A domain-PIP<sub>2</sub> interaction may be involved in the distribution of plasmalemmal DAT. In contrast, syntaxin 1A and synaptophysin, the integral membrane proteins, were almost completely recovered in soluble cytosolic fraction, but not in a detergent-resistant fraction. Rim 2, a scaffolding protein with C<sub>2</sub> domain, is known to interact with Piccolo and to regulate presynaptic events. However, its similar subdistribution in the three fractions was different from that of Piccolo C<sub>2</sub>A domain. To get an insight into the interplay among DAT, Piccolo C<sub>2</sub>A domain and PIP<sub>2</sub>, double immunostaining was performed. We found that Piccolo C<sub>2</sub>A domain mainly anchored nonuniformly to the inner leaflet of plasma membrane (Figure 5e), which is consistent with its property of targeting membrane PIP<sub>2</sub>. Notably, the distribution pattern of C<sub>2</sub>A domain resembled that of hDAT, as revealed by the paralleled immunoreactivities at membrane microdomains (Figure 5f).

*Internalization of plasmalemmal DAT is PIP<sub>2</sub>-dependent*

The concept of PIP<sub>2</sub> as a spatially localized regulator of membrane trafficking is clearly illustrated by its key role in clathrin-mediated endocytosis for transporter. If plasmalemmal DAT is triggered to internalize by METH, it should be accompanied by PIP<sub>2</sub> for recruiting endocytic adaptors through PIP<sub>2</sub>-binding modules. To test this idea, hDAT and PIP<sub>2</sub> were double-stained in hDAT-PC12 cells after treatment of saline or 1 μM METH for 30 min. Surprisingly, the internalized DAT triggered by METH was found to colocalize with the PIP<sub>2</sub> in the cytosolic compartment (Figure 6, bottom panel), whereas the saline-treated cells only showed the constitutively internalized PIP<sub>2</sub> and DAT (Figure 6, top panel). These results further demonstrated that DAT internalization is also a clathrin-dependent process requiring the assembly of endocytic components like PIP<sub>2</sub>.

*Interaction of Piccolo C<sub>2</sub>A domain and PIP<sub>2</sub>*

Although Piccolo C<sub>2</sub>A domain binding to PIP<sub>2</sub> has been demonstrated using artificial membranes,<sup>15</sup> there is no evidence indicating interaction of the two molecules in living models. We first investigated whether plasmalemmal clusters of Piccolo immunoreactivity coincide with sites of local PIP<sub>2</sub> accumulation using double immunostaining. The clusters of Piccolo immunoreactivities in dendrite profile colocalized precisely with those of PIP<sub>2</sub> in the primary cultured dopaminergic neurons (Figure 7a). Moreover, the localization of transfected C<sub>2</sub>A domain in hDAT-PC12 cells was similar with that of PIP<sub>2</sub>, which revealed a patchy staining pattern at plasma membrane (Figure 7b). Importantly, the clusters with strong immunoreactivity of C<sub>2</sub>A domain also showed substantially larger and stronger labeling macroscopic of PIP<sub>2</sub> clusters, indicating that C<sub>2</sub>A domain may sequester PIP<sub>2</sub>, thus augmenting the formation of microscopically detectable plasmalemmal PIP<sub>2</sub> clusters.

To better understand the interaction of the two molecules, we generated a PIs binding model of Piccolo C<sub>2</sub>A domain with Ca<sup>2+</sup> docking. As show in Figure 7c, the three-dimensional structure indicated that the predicted PIs binding sites are Ca<sup>2+</sup>-binding loops at the top of C<sub>2</sub>A domain, which shows the similar binding residues for phosphatidylinositol (PI), phosphatidylinositol 4-phosphate (PIP) and PIP<sub>2</sub>. Notably, the crystal packing contacts for PIP<sub>2</sub> were the clusters of basic/aromatic residues including 4668–4670 (DNN), 4697–4698 (QK), 4738–4743 (DYDRFS) and 4746 (D). The potential importance of these residues is highlighted by the fact that they are completely conserved among rat, mouse, human and chicken Piccolo.<sup>22</sup> Calculation of the electrostatic surface potential of C<sub>2</sub>A domain showed that PIP<sub>2</sub> binding sites are positively charged (Figure 7d), further indicating that clustering PIs by C<sub>2</sub>A domain depends on electrostatic interactions between the

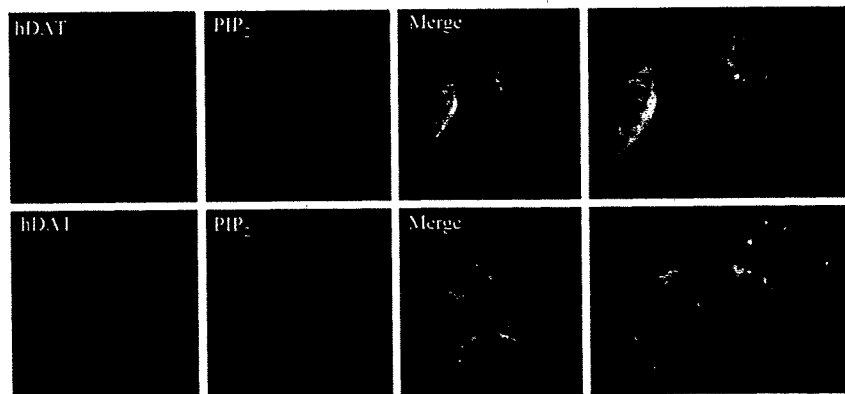


**Figure 6** Piccolo C<sub>2</sub>A domain attenuates dopamine transporter (DAT) internalization responding to methamphetamine (METH). Double-immunostaining of PIP<sub>2</sub> (red) and hDAT (green) in hDAT-PC12 cells. The internalization of hDAT was promoted by METH, which is accompanied by PIP<sub>2</sub> (bottom panel). The saline-treated cells show strong immunoreactivities of both hDAT and PIP<sub>2</sub> (top panel).

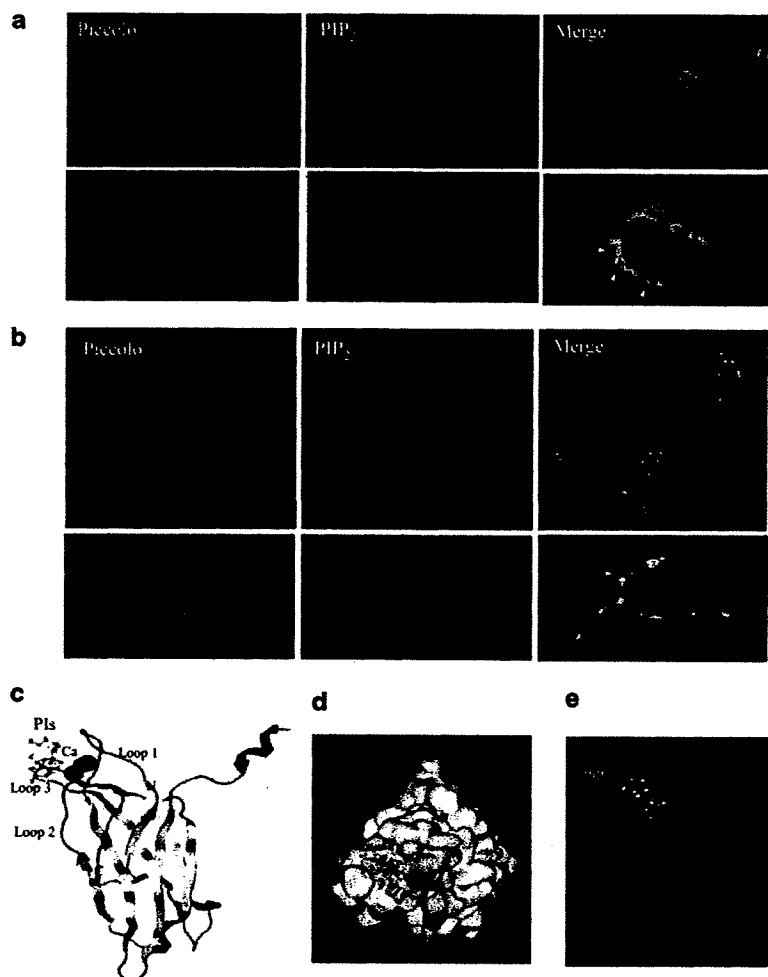


**Figure 7** Interaction of Piccolo and PIP<sub>2</sub>. (a) PIP<sub>2</sub> (red) colocalizes precisely with Piccolo (green) along the presynaptic terminal in primary cultured dopaminergic neurons (arrowed). (b) PIP<sub>2</sub> (red) accumulates at plasmalemmal rafts, where it colocalizes with Piccolo (green) in hDAT-PC12 cells. Arrowheads point to regions of intense staining of PIP<sub>2</sub> and Piccolo. (c) Model of Piccolo C<sub>2</sub>A domain with three bound Ca<sup>2+</sup> ions on top (green spheres). The top surface of C<sub>2</sub>A domain shows the binding sites for the headgroups of PIs. (d) Surface plot showing the electrostatic potential of C<sub>2</sub>A domain. Blue, positive; red, negative charge; white, neutral. PIP<sub>2</sub> is pointed. (e) Space-filling model of PIP<sub>2</sub> is shown on top in pink C<sub>2</sub>A domain, which provides a cupped shape of polybasic region to accommodate PIP<sub>2</sub>.

positively charged residues in proteins and the negatively charged headgroups of PIs. The lowest binding energies of Piccolo C<sub>2</sub>A domain for PI, PIP and PIP<sub>2</sub> with Ca<sup>2+</sup> docking were -59.491, -93.229 and -102.642 Kcal, respectively, suggesting a specific interaction between PIP<sub>2</sub> and C<sub>2</sub>A domain. Furthermore, the space-filling model showed that PIP<sub>2</sub> is tightly packed against the top surface of C<sub>2</sub>A domain, which forms a favorable pocket to accommodate the moiety of PIP<sub>2</sub> (Figure 7e).

*Piccolo regulated DAT function not through syntaxin 1A*  
As syntaxin 1A has been demonstrated to regulate the expressions and activities of serotonin transporter (SERT) and  $\gamma$ -aminobutyric acid (GABA) transporters,<sup>23,24</sup> Piccolo might regulate DAT surface

expression through interaction with syntaxin 1A. We first investigated whether syntaxin 1A could bind to Piccolo, though syntaxin is identified to bind to Piccolo.<sup>25</sup> The lysates from hDAT-PC12 cells were immunoprecipitated with anti-syntaxin 1A, followed by hDAT immunoblotting. As shown in Supplementary Figure 1a, hDAT were present in the lysate. As expected, we also detected co-immunoprecipitation of hDAT and syntaxin 1A in following immunoprecipitation with anti-hDAT (Supplementary Figure 1b). These results showed an apparent association of these two molecules, which was supported by previous reports.<sup>26</sup> We then investigated whether syntaxin 1A could regulate DAT activity. The hDAT-PC12 cells were pretreated with Bont/C1, a toxin that specifically cleaves syntaxin 1A, followed by



[<sup>3</sup>H]DA uptake assay; moreover, Bont/B that specifically cleaves the vesicle *N*-ethylmaleimide-sensitive factor attachment receptor protein synaptobrevin was used as a control. As shown in Supplementary Figure 1c, Bont/C1 (0.5–5 nM) failed to alter the [<sup>3</sup>H]DA uptake in the cells treated with saline. Although Bont/C1 slightly elevated [<sup>3</sup>H]DA uptake in the cells exposed to METH compared with Bont/B, the difference was not significant. To exclude that such incapability of Bont/C1 in modulating DA uptake was a result of the low concentration or short exposure time, we treated the cells with Bont/C1 at 0.25 μM for 6 h. However, [<sup>3</sup>H]DA uptake was also not altered (data not shown). Additionally, exposure of METH at the concentration ranging from 0.5–20 μM for 30 min did not alter the expression level of syntaxin 1A in hDAT-PC12 cells (data not shown). Taken together, these data suggest that DAT and syntaxin 1A may mechanically, but not functionally, interact. Given the incapability of syntaxin 1A itself in modulating DAT, it unlikely mediates the role of Piccolo in regulating DAT expression at plasma membrane.

## Discussion

The contribution of dopaminergic transmission to behavioral sensitization has been well recognized. Expression of certain proteins appears to be compensatory adaptation to the excessive DA signaling, which could be biologically adaptive mechanisms contributing to addiction. Nevertheless, some proteins likely function in a reverse manner. For example, we have previously found that the expression of tissue plasminogen activator plays a positive role in morphine-induced synaptic plasticity,<sup>19</sup> whereas tumor necrosis factor- $\alpha$  expression in NAC inhibits METH-induced dependence.<sup>18</sup> Piccolo expression was upregulated by repeated METH administration and partial knockdown of Piccolo expression by antisense technique led to elevated synaptic DA concentration in the NAC and two major behavioral manifestations in mice: heightened hyperlocomotor activity and rewarding effect. These findings strongly show that Piccolo overexpression elicited by METH may serve as a homeostatic mechanism that prevents behavioral sensitization by maintaining the expression and activity of the plasmalemmal DAT.

The human Piccolo gene contains more than 25 exons spanning over 350 kb of genomic DNA maps to 7q11.23-q21.3, a region of chromosome 7 implicated as a linkage site for autism and Williams Syndrome.<sup>22</sup> Therefore, dysfunction of Piccolo may be involved in cognitive impairment and mental retardation.<sup>27</sup> The mechanism underlying Piccolo upregulation caused by METH remains to be elucidated. Nevertheless, inhibitory feedback to the excessive DA signaling would be a plausible candidate.

Piccolo has been reported to localize at the GABAergic and glycinergic presynaptic terminal,<sup>10</sup> and our findings in immunostaining demonstrated

that it is also expressed at dopaminergic presynaptic terminal. DAT can be internalized from the plasma membrane at a relatively rapid rate, which provides a mechanism by which the turnover rate and density of the plasmalemmal DAT can be quickly and finely modulated.<sup>6,8</sup> Signaling molecules, glycosylation and DAT substrates have been shown to regulate DAT membrane trafficking. Given those findings *in vivo* behaviors tests and the properties of Piccolo, we assumed that Piccolo may play a role in modulating DA flux and DAT distribution at dopaminergic terminals. To address this issue, we investigated DA uptake and membrane DAT expression in hDAT-PC12 cells expressing different functional domain of Piccolo. METH caused DA uptake inhibition in parallel with decreased DAT surface expression, which was well consistent with those works defining the dynamically internalized DAT in hDAT-PC12 cells triggered by amphetamine. These results further support the notion that redistribution of surface DAT caused by METH-like drugs may present an important mechanism underlying the consequently reduced DAT activity. Our data showed that Piccolo C<sub>2</sub>A, but not PDZ domain, attenuated METH-induced DA uptake inhibition by retaining DAT expression at cell surface. Because DAT can be internalized and/or recycled, we speculated that the decreased loss of membrane DAT could be resulted from attenuated DAT internalization. Such hypothesis was demonstrated by reversible biotinylation, which revealed the decreased DAT internalization in C<sub>2</sub>A domain-transfected cells responding to METH.

It is well established that PIP<sub>2</sub> functions in regulating cytoskeleton, channels and transporters, and membrane trafficking at presynaptic terminal.<sup>16,28,29</sup> Especially, PIP<sub>2</sub> is essential at several stages of endocytosis for the sequential recruitment of adaptor and accessory proteins to endocytic sites.<sup>30,31</sup> METH rapidly causes both DAT internalization and conformational rearrangement to an intracellularly oriented transporter from which DA is released. Such process is proposed to be a drastic membrane movement and requires PIP<sub>2</sub> to assemble various molecules to form endocytic compartment. Significantly, we found that PIP<sub>2</sub> exhibits a similar distribution pattern with DAT at membrane microdomains. Furthermore, internalized DTA triggered by METH is accompanied with PIP<sub>2</sub> in endocytic compartments. These results indicate that PIP<sub>2</sub> is an important regulator in the process of DAT internalization.

A couple of scaffolding proteins such as GAP43, CAP23 and Dap160 have shown their ability to sequester membrane PIP<sub>2</sub>, thus potentially modulating the endocytic process.<sup>32,33</sup> In this study we obtained several evidences further supporting the notion that Piccolo can electrostatically sequester PIP<sub>2</sub>. Firstly, Piccolo C<sub>2</sub>A domain may laterally bind membrane PIP<sub>2</sub>, and augment PIP<sub>2</sub> clusters in hDAT-PC12 cells. In principle, the augmented clusters could represent the sequestration of phospholipids like PIP<sub>2</sub> at the plasma membrane.<sup>34</sup> Secondly, the crystal

packing contacts for PIP<sub>2</sub> were the clusters of basic/aromatic residues, which exhibit a universal capability of sequestering membrane PIP<sub>2</sub>.<sup>35</sup> Thirdly, the space-filling model showed that Piccolo C<sub>2</sub>A domain may pocket PIP<sub>2</sub> by a cupped shape of polybasic region, where the local positive potential electrostatically attracts the negatively charged PIP<sub>2</sub>. Finally, C<sub>2</sub>A domain shows stronger interacting potential with PIP<sub>2</sub> than PI or PIP. Our results are consistent with previous investigations indicating that PIs binding with Piccolo C<sub>2</sub>A domain is largely driven by electrostatic interaction.<sup>15</sup>

Based on these findings, we speculated that Piccolo C<sub>2</sub>A domain may regulate METH-triggered DAT internalization through sequestering PIP<sub>2</sub>, and the findings in immunostaining strongly support this prediction. Piccolo C<sub>2</sub>A domain mainly anchors nonuniformly to the inner leaflet, which is accompanied with the retention of DAT and PIP<sub>2</sub> at membrane microdomains; moreover, it clearly attenuated METH-triggered DAT and PIP<sub>2</sub> internalization in cytosol. These results show that Piccolo may sequester or 'control' locally PIP<sub>2</sub> by C<sub>2</sub>A domain in membrane raft and suppress PIP<sub>2</sub>-dependent endocytic process, thus leading to the attenuated DAT internalization.

How does the Piccolo C<sub>2</sub>A domain-PIP<sub>2</sub> interaction fulfill a function in modulating DAT internalization and psychostimulant responsiveness? An explanation could be that the endocytic process for DAT internalization is inhibited directly through PIP<sub>2</sub> sequestration. Given the strong dependence of the endocytic machinery on PIP<sub>2</sub>, more membrane PIP<sub>2</sub> is considerably mobilized for the accelerated DAT internalization triggered by METH. This situation would place the endocytic machinery of dopaminergic presynaptic terminal in a compromised position of insufficient availability of PIP<sub>2</sub>, and thus slowing down the DAT internalization. Similarly, a dominant-negative mutant of dynamin I, a component of endocytic machinery, inhibits both PKC- and amphetamine-dependent DAT internalization,<sup>7,36</sup> interruption of adaptor proteins present in clathrin-coated pits like epsin interferes with DAT endocytosis.<sup>37</sup> Another explanation could be that Piccolo C<sub>2</sub>A domain may retain DAT at cell surface by promoting membrane stability. METH causes both DAT internalization and conformational rearrangement to an intracellularly oriented transporter from which DA is released. In this process PIP<sub>2</sub> acts as a positive regulator in modulating actin filament assembly and membrane movement by creating membrane microdomains and binding proteins with lipid-specific interaction.<sup>38,39</sup> Therefore, overexpressed Piccolo elicited by METH may enhance the association with membrane PIP<sub>2</sub> or other PIs through C<sub>2</sub>A domain and disturb PIP<sub>2</sub>-dependent actin assembly, thereby strengthening membrane stability and weakening DAT internalization. In this case, Piccolo may function as a general stabilizer for plasma membrane and DAT. It is worth noting that protein interacting with C kinase 1 (PICK1), a skeletal

component, may also stabilize and maintain DAT at plasma membrane.<sup>40</sup>

Piccolo likely binds to syntaxin 1A through its C<sub>2</sub>A domain, because synaptotagmin C<sub>2</sub>A domain which shares a great structural similarity with Piccolo C<sub>2</sub>A domain interacts with syntaxin 1A.<sup>15,40</sup> Syntaxin 1A directly regulates the expressions and activities of SERT and GABA transporter.<sup>23,24</sup> Interestingly, a recent work has identified that syntaxin 1A also binds to DAT.<sup>26</sup> However, Piccolo C<sub>2</sub>A domain appears not to regulate METH-induced DAT internalization through syntaxin 1A, because DA uptake is not affected when syntaxin 1A is inhibited.

Our findings reveal that Piccolo is capable of regulating METH-induced DAT internalization, leading to the change of DA signaling and synaptic strength. The precise mechanism underlying the role of C<sub>2</sub>A domain-PIP<sub>2</sub> interplay in DAT internalization remains to be determined. No matter which mechanism could be more reasonable, sequestration of PIP<sub>2</sub> in lateral domains through C<sub>2</sub>A domain appears to be important for Piccolo to regulate DAT internalization. Therefore, a greater understanding of the molecular regulators for PIP<sub>2</sub>, which governs DAT trafficking, would shed light on the modulation of DAT surface presentation. Further investigation measuring membrane fluorescence resonance energy transfer and PIP<sub>2</sub> turnover/mobilization will help interpret the contribution of the proposed mechanisms.

The present investigation illustrates a paradigm that Piccolo, a presynaptic scaffolding protein, targets membrane PIP<sub>2</sub> by its C<sub>2</sub>A domain, contributing to the regulation of DAT internalization. Piccolo upregulation may represent a homeostatic response of dopaminergic neurons in the NAc to excessive dopaminergic transmission, dampening hypersensitivity and rewarding effect.

#### Acknowledgments

We are thankful to Dr Seino Susumu and Dr Shibusaki Takao (Division of Cellular and Molecular Medicine, Kobe University Graduate School of Medicine, Japan) for the kind gifts of pCMV-HA-Piccolo-PDZ, pCMV-Myc-Piccolo-C<sub>2</sub>A and pGEX4T-GST-p13192. We thank Mrs Nobushi Hamada and Yoshiyuki Nakamura radioisotope Center Medical Branch, Nagoya University School of Medicine for technical support. This study was supported in part by a Grant-in-Aid for Science Research and Special Coordination Funds for Promoting Science and Technology, Target-Oriented Brain Science Research Program and 21st Century Center of Excellence Program 'Integrated Molecular Medicine for Neuronal and Neoplastic Disorders' and 'Academic Frontier Project for Private Universities (2007-2011)', from the Ministry of Education, Culture, Sports, Science and Technology of Japan; by a Grant-in-Aid for Health Science Research on Regulatory Science of Pharmaceuticals and Medical Devices, and Comprehensive Research on Aging and Health from the

Ministry of Health, Labor and Welfare of Japan; by a Smoking Research Foundation Grant for Biomedical Research and Takeda Science Foundation.

## References

- 1 Kahlig KM, Binda F, Khoshbouei H, Blakely RD, McMahon DG, Javitch JA *et al*. Amphetamine induces dopamine efflux through a dopamine transporter channel. *Proc Natl Acad Sci USA* 2005; **102**: 3495–3500.
- 2 Sulzer D, Chen TK, Lau YY, Kristensen H, Rayport S, Ewing A. Amphetamine redistributes dopamine from synaptic vesicles to the cytosol and promotes reverse transport. *J Neurosci* 1995; **15**: 4102–4108.
- 3 Sandoval V, Riddle EL, Ugarte YV, Hanson GR, Fleckenstein AE. Methamphetamine-induced rapid and reversible changes in dopamine transporter function: an *in vitro* model. *J Neurosci* 2001; **21**: 1413–1419.
- 4 Holton KL, Loder MK, Melikian HE. Nonclassical, distinct endocytic signals dictate constitutive and PKC-regulated neurotransmitter transporter internalization. *Nat Neurosci* 2005; **8**: 881–888.
- 5 Sorkina T, Hoover BR, Zahniser NR, Sorkin A. Constitutive and protein kinase C-induced internalization of the dopamine transporter is mediated by a clathrin-dependent mechanism. *Traffic* 2005; **6**: 157–170.
- 6 Loder MK, Melikian HE. The dopamine transporter constitutively internalizes and recycles in a protein kinase C-regulated manner in stably transfected PC12 cell lines. *J Biol Chem* 2003; **278**: 22168–22174.
- 7 Saunders C, Ferrer JV, Shi L, Chen J, Merrill G, Lamb ME *et al*. Amphetamine-induced loss of human dopamine transporter activity: an internalization-dependent and cocaine-sensitive mechanism. *Proc Natl Acad Sci USA* 2000; **97**: 6850–6855.
- 8 Sorkina T, Doolen S, Galperin E, Zahniser NR, Sorkin A. Oligomerization of dopamine transporters visualized in living cells by fluorescence resonance energy transfer microscopy. *J Biol Chem* 2003; **278**: 28274–28283.
- 9 Zhai RG, Vardinon-Friedman H, Cases-Langhoff C, Becker B, Gundelfinger ED, Ziv NE *et al*. Assembling the presynaptic active zone: a characterization of an active one precursor vesicle. *Neuron* 2001; **29**: 131–143.
- 10 Fenster SD, Chung WJ, Zhai R, Cases-Langhoff C, Voss B, Garner AM *et al*. Piccolo, a presynaptic zinc finger protein structurally related to bassoon. *Neuron* 2000; **25**: 203–214.
- 11 Fenster SD, Kessels MM, Qualmann B, Chung WJ, Nash J, Gundelfinger ED *et al*. Interactions between Piccolo and the actin/dynamin-binding protein Abp1 link vesicle endocytosis to presynaptic active zones. *J Biol Chem* 2003; **278**: 20268–20277.
- 12 Wang X, Kibschull M, Laue MM, Lichte B, Petrasch-Parwez E, Kilimann MW. Aczonin, a 550-kD putative scaffolding protein of presynaptic active zones, shares homology regions with Rim and Bassoon and binds profilin. *J Cell Biol* 1999; **147**: 151–162.
- 13 Garner CC, Nash J, Hagan RL. PDZ domains in synapse assembly and signaling. *Trends Cell Biol* 2000; **10**: 274–280.
- 14 Garcia J, Gerber SH, Sugita S, Sudhof TC, Rizo J. A conformational switch in the Piccolo C2A domain regulated by alternative splicing. *Nat Struct Mol Biol* 2004; **11**: 45–53.
- 15 Gerber SH, Garcia J, Rizo J, Sudhof TC. An unusual C(2)-domain in the active-zone protein piccolo: implications for Ca(2+) regulation of neurotransmitter release. *EMBO J* 2001; **20**: 1605–1619.
- 16 Cremona O, De Camilli P. Phosphoinositides in membrane traffic at the synapse. *J Cell Sci* 2001; **114**: 1041–1052.
- 17 Fujimoto K, Shibasaki T, Yokoi N, Kashima Y, Matsumoto M, Sasaki T *et al*. Piccolo, a Ca<sup>2+</sup> sensor in pancreatic beta-cells. Involvement of cAMP-GEFII.Rim2.Piccolo complex in cAMP-dependent exocytosis. *J Biol Chem* 2002; **277**: 50497–50502.
- 18 Nakajima A, Yamada K, Nagai T, Uchiyama T, Miyamoto Y, Mamiya T *et al*. Role of tumor necrosis factor-alpha in methamphetamine-induced drug dependence and neurotoxicity. *J Neurosci* 2004; **24**: 2212–2225.
- 19 Nagai T, Yamada K, Yoshimura M, Ishikawa K, Miyamoto Y, Hashimoto K *et al*. The tissue plasminogen activator-plasmin system participates in the rewarding effect of morphine by regulating dopamine release. *Proc Natl Acad Sci USA* 2004; **101**: 3650–3655.
- 20 Melikian HE, Buckley KM. Membrane trafficking regulates the activity of the human dopamine transporter. *J Neurosci* 1999; **19**: 7699–7710.
- 21 Bowers MS, McFarland K, Lake RW, Peterson YK, Lapish CC, Gregory ML *et al*. Activator of G protein signaling 3: a gatekeeper of cocaine sensitization and drug seeking. *Neuron* 2004; **42**: 269–281.
- 22 Fenster SD, Garner CC. Gene structure and genetic localization of the PCLO gene encoding the presynaptic active zone protein Piccolo. *Int J Dev Neurosci* 2002; **20**: 161–171.
- 23 Quick MW. Regulating the conducting states of a mammalian serotonin transporter. *Neuron* 2003; **40**: 537–549.
- 24 Deken SL, Beckman ML, Boos L, Quick MW. Transport rates of GABA transporters: regulation by the N-terminal domain and syntaxin 1A. *Nat Neurosci* 2002; **3**: 998–1003.
- 25 Shapira M, Zhai RG, Dresbach T, Bresler T, Torres VI, Gundelfinger ED *et al*. Unitary assembly of presynaptic active zones from Piccolo-Bassoon transport vesicles. *Neuron* 2003; **38**: 237–252.
- 26 Lee KH, Kim MY, Kim DH, Lee YS. Syntaxin 1A and receptor for activated C kinase interact with the N-terminal region of human dopamine transporter. *Neurochem Res* 2004; **29**: 1405–1409.
- 27 Weidenhofer J, Bowden NA, Scott RJ, Tooney PA. Altered gene expression in the amygdala in schizophrenia: up-regulation of genes located in the cytomatrix active zone. *Mol Cell Neurosci* 2006; **31**: 243–250.
- 28 Suh BC, Hille B. Regulation of ion channels by phosphatidylinositol 4,5-bisphosphate. *Curr Opin Neurobiol* 2005; **15**: 370–378.
- 29 Kanzaki M, Furukawa M, Raab W, Pessin JE. Phosphatidylinositol 4,5-bisphosphate regulates adipocyte actin dynamics and GLUT4 vesicle recycling. *J Biol Chem* 2004; **279**: 30622–30633.
- 30 Slepnev VI, De Camilli P. Accessory factors in clathrin-dependent synaptic vesicle endocytosis. *Nat Rev Neurosci* 2000; **1**: 161–172.
- 31 Itoh T, Koshiba S, Kigawa T, Kikuchi A, Yokoyama S, Takenawa T. Role of the ENTH domain in phosphatidylinositol-4,5-bisphosphate binding and endocytosis. *Science* 2001; **291**: 1047–1051.
- 32 Laux T, Fukami K, Thelen M, Golub T, Frey D, Caroni P. GAP43, MARCKS, and CAP23 modulate PI(4,5)P(2) at plasmalemmal rafts, and regulate cell cortex actin dynamics through a common mechanism. *J Cell Biol* 2000; **86**: 2188–2207.
- 33 Marie B, Sweeney ST, Poskanzer KE, Roos J, Kelly RB, Davis GW. Dap160/intersectin scaffolds the periactional zone to achieve high-fidelity endocytosis and normal synaptic growth. *Neuron* 2004; **43**: 207–219.
- 34 Kwik J, Boyle S, Fooksman D, Margolis L, Sheetz MP, Eddin M. Membrane cholesterol, lateral mobility, and the phosphatidylinositol 4,5-bisphosphate-dependent organization of cell actin. *Proc Natl Acad Sci USA* 2003; **100**: 13964–13969.
- 35 Daniels GM, Amara SG. Regulated trafficking of the human dopamine transporter-clathrin-mediated internalization and lysosomal degradation in response to phorbol esters. *J Biol Chem* 1999; **274**: 35794–35801.
- 36 Sorkina T, Miranda M, Dionne KR, Hoover BR, Zahniser NR, Sorkin A. RNA interference screen reveals an essential role of Nedd4-2 in dopamine transporter ubiquitination and endocytosis. *J Neurosci* 2006; **26**: 8195–8205.
- 37 Nebel T, Oh SW, Luna EJ. Membrane cytoskeleton: PIP(2) pulls the strings. *Curr Biol* 2000; **10**: R351–R354.
- 38 Gruenberg J. Lipids in endocytic membrane transport and sorting. *Curr Opin Cell Biol* 2003; **15**: 382–388.
- 39 Torres GE, Yao WD, Mohn AR, Quan H, Kim KM, Levey AI *et al*. Functional interaction between monoamine plasma membrane transporters and the synaptic PDZ domain-containing protein PICK1. *Neuron* 2001; **30**: 121–134.
- 40 Shao X, Li C, Fernandez I, Zhang X, Sudhof TC, Rizo J. Synaptotagmin-syntaxin interaction: the C2 domain as a Ca<sup>2+</sup>-dependent electrostatic switch. *Neuron* 1997; **18**: 133–142.

Supplementary Information accompanies the paper on the Molecular Psychiatry website (<http://www.nature.com/mp>)

# Aripiprazole ameliorates phencyclidine-induced impairment of recognition memory through dopamine D<sub>1</sub> and serotonin 5-HT<sub>1A</sub> receptors

Taku Nagai · Rina Murai · Kanae Matsui ·  
Hiroyuki Kamei · Yukihiro Noda · Hiroshi Furukawa ·  
Toshitaka Nabeshima

Received: 10 March 2008 / Accepted: 13 June 2008  
© Springer-Verlag 2008

## Abstract

**Rationale** Cognitive deficits, including memory impairment, are regarded as a core feature of schizophrenia. Aripiprazole, an atypical antipsychotic drug, has been shown to improve disruption of prepulse inhibition and social interaction in an animal model of schizophrenia induced by phencyclidine (PCP); however, the effects of aripiprazole on recognition memory remain to be investigated.

**Electronic supplementary material** The online version of this article (doi:10.1007/s00213-008-1240-6) contains supplementary material, which is available to authorized users.

T. Nagai · T. Nabeshima  
Department of Neuropsychopharmacology and Hospital  
Pharmacy, Nagoya University Graduate School of Medicine,  
Nagoya, Japan

R. Murai · T. Nabeshima (✉)  
Department of Chemical Pharmacology,  
Graduate School of Pharmaceutical Sciences, Meijo University,  
150 Yagotoyama, Tenpaku-ku,  
Nagoya 468-8503, Japan  
e-mail: tnabeshi@ccmfs.meijo-u.ac.jp

K. Matsui · H. Kamei  
Department of Health-Care Pharmacy,  
Graduate School of Pharmaceutical Sciences, Meijo University,  
Nagoya, Japan

Y. Noda  
Division of Clinical Science in Clinical Pharmacy Practice,  
Graduate School of Pharmaceutical Sciences, Meijo University,  
Nagoya, Japan

H. Furukawa  
Department of Medical Chemistry,  
Graduate School of Pharmaceutical Sciences, Meijo University,  
Nagoya, Japan

**Objectives** In this study, we examined the effect of aripiprazole on cognitive impairment in mice treated with PCP repeatedly.

**Materials and methods** Mice were repeatedly administered PCP at a dose of 10mg/kg for 14days, and their cognitive function was assessed using a novel-object recognition task. We investigated the therapeutic effects of aripiprazole (0.01–1.0mg/kg) and haloperidol (0.3 and 1.0mg/kg) on cognitive impairment in mice treated with PCP repeatedly. **Results** Single (1.0mg/kg) and repeated (0.03 and 0.1mg/kg, for 7days) treatment with aripiprazole ameliorated PCP-induced impairment of recognition memory, although single treatment significantly decreased the total exploration time during the training session. In contrast, both single and repeated treatment with haloperidol (0.3 and 1.0mg/kg) failed to attenuate PCP-induced cognitive impairment. The ameliorating effect of aripiprazole on recognition memory in PCP-treated mice was blocked by co-treatment with a dopamine D<sub>1</sub> receptor antagonist, SCH23390, and a serotonin 5-HT<sub>1A</sub> receptor antagonist, WAY100635; however, co-treatment with a D<sub>2</sub> receptor antagonist raclopride had no effect on the ameliorating effect of aripiprazole.

**Conclusions** These results suggest that the ameliorative effect of aripiprazole on PCP-induced memory impairment is associated with dopamine D<sub>1</sub> and serotonin 5-HT<sub>1A</sub> receptors.

**Keywords** Aripiprazole · Dopamine D<sub>1</sub> receptor · Memory · Phencyclidine · Serotonin 5-HT<sub>1A</sub> receptor

## Introduction

Schizophrenia is a devastating psychiatric disorder that impairs mental and social functioning and affects approx-

imately 1% of the population worldwide (Rössler et al. 2005). Typical symptoms can be separated into positive symptoms (e.g., hallucinations, delusions, and thought disorder), negative symptoms (e.g., deficits in social interaction, emotional expression, and motivation), and cognitive dysfunction (e.g., impaired attention/information processing, problem-solving, processing speed, verbal and visual learning, and memory and working memory) (Nuechterlein et al. 2004; Pearlson 2000). Pharmacological treatment of schizophrenia is available. First-generation (typical) antipsychotics alleviate psychotic symptoms, but lead to severe motor side effects through the blockade of dopamine D<sub>2</sub> receptors (Kapur et al. 2000). Second-generation (atypical) antipsychotics have improved tolerability and milder motor side effects than typical antipsychotics but induce weight gain and metabolic disturbances (Newcomer 2005). Despite appropriate treatment with either typical antipsychotics or atypical antipsychotics, schizophrenic patients continue to exhibit pronounced cognitive impairment (Keefe et al. 2007; Mishara and Goldberg 2004; Woodward et al. 2005).

Aripiprazole, 7-(4-[4-(2,3-dichlorophenyl)-1-piperazinyl]butyloxy)-3,4-dihydro- carbostyil, is a novel atypical antipsychotic drug that differs from other typical and atypical antipsychotics, improving both positive and negative symptoms of psychosis without producing extrapyramidal side effects or increases in serum prolactin (DeLeon et al. 2004; Tamminga 2002). It has been demonstrated that aripiprazole has high affinity for a large number of monoaminergic receptors, including dopamine D<sub>2</sub>, serotonin 5-HT<sub>1A</sub>, and 5-HT<sub>2A</sub> receptors (Green 2004; Shapiro et al. 2003) and acts as a partial dopamine D<sub>2</sub> receptor agonist (Kikuchi et al. 1995), a partial 5-HT<sub>1A</sub> receptor agonist (Jordan et al. 2002), and as an 5-HT<sub>2A</sub> receptor antagonist (McQuade et al. 2002). These pharmacological properties may play a role in the therapeutic effects of aripiprazole. Although aripiprazole has been reported to enhance cognitive function in schizophrenia (Rivas-Vasquez 2003), the mechanism of the improving effect of aripiprazole on cognitive impairment is unclear.

Phencyclidine [1-(1-phenylcyclohexyl) piperidine hydrochloride (PCP)], a noncompetitive *N*-methyl-D-aspartate receptor antagonist, has been shown to induce schizophrenia-like psychosis, presenting as positive symptoms, negative symptoms, and cognitive deficits in humans (Javitt and Zukin 1991), which persist several weeks after withdrawal of chronic PCP use (Allen and Young 1978; Lerner and Burns 1986; Rainey and Crowder 1975). To investigate the pathophysiology of schizophrenia, an animal model of schizophrenia was established using PCP (Mouri et al. 2007a). We have previously demonstrated that repeated treatment with PCP (10mg/kg/day s.c. for 14days) induces several schizophrenia-like behavioral abnormalities, such as

increased immobility in a forced swimming test (Murai et al. 2007; Noda et al. 1995, 1997, 2000), social deficits in a social interaction test (Qiao et al. 2001), impairment of latent learning in a water finding test (Mouri et al. 2007b), and associative learning impairment in cued and contextual fear conditioning tests (Enomoto et al. 2005) in mice. Moreover, it has been reported that PCP induces the disruption of sensorimotor gating in a prepulse inhibition test (Bakshi et al. 1994) and recognition memory in a novel object recognition test (Hashimoto et al. 2005); therefore, PCP-treated mice might be a useful animal model of schizophrenia.

There are a few reports suggesting the effectiveness of aripiprazole on cognitive dysfunction and negative symptoms in PCP-treated animals. For example, aripiprazole improves PCP-induced disruption of prepulse inhibition (Fejgin et al. 2007) and social interaction (Bruins Slot et al. 2005) in mice and rats, respectively; however, the effects of aripiprazole on recognition memory remain to be investigated. In this study, we examined whether aripiprazole improves PCP-induced cognitive impairment in a novel object recognition test in mice.

## Materials and methods

### Animals

Male ICR mice (7weeks old) were obtained from Nihon SLC (Shizuoka, Japan). The animals were housed in plastic cages and kept in a regulated environment (23 ± 1°C, 50 ± 5% humidity), with a 12/12h light–dark cycle (lights on at 09:00hours). Food (CE2; Clea Japan, Tokyo, Japan) and tap water were available ad libitum. All animal care and use were in accordance with the National Institutes of Health Guide for the Care and Use of Laboratory Animals and were approved by the Institutional Animal Care and Use Committee of Nagoya University.

### Drugs

PCP hydrochloride was synthesized by the authors according to the method of Maddox et al. (1965) and was checked for purity. Aripiprazole was provided by Otsuka Pharmaceutical (Tokyo, Japan). SCH23390 hydrochloride, *S*(-)-raclopride (+)-tartrate, haloperidol and WAY100635 were purchased from Sigma-Aldrich (St. Louis, MO, USA). The dose of each drug refers to previous reports (Noda et al. 1995; Bruins Slot et al. 2005; Kamei et al. 2006; Ito et al. 2007b).

PCP was dissolved in saline. SCH23390, raclopride, and WAY100635 was dissolved in distilled water. Aripiprazole and haloperidol were suspended in saline containing 0.1% carboxymethylcellulose (CMC) sodium salt. All drugs were administered in a volume of 0.1ml/10g body weight.